NACA

RESEARCH MEMORANDUM

AN INVESTIGATION OF THE CHARACTERISTICS OF THREE NACA 1-SERIES NOSE INLETS AT SUBCRITICAL AND SUPERCRITICAL MACH NUMBERS

By

Robert E. Pendley and Norman F. Smith

Langley Aeronautical Laboratory
Langley Field, Va.

NATIONAL ADVISORY COMMITTEE FOR AERONAUTICS

WASHINGTON

January 13, 1949

NACA RM No. L8L06

NATIONAL ADVISORY COMMITTEE FOR AERONAUTICS

RESEARCH MEMORANDUM

AN INVESTIGATION OF THE CHARACTERISTICS OF THREE NACA 1-SERIES NOSE INLETS AT SUBCRITICAL AND SUPERCRITICAL MACH NUMBERS

By Robert E. Pendley and Norman F. Smith

SUMMARY

An investigation of the characteristics of three representative NACA 1-series nose inlets over a Mach number range extending from 0.4 to 0.925 has been performed in the Langley 8-foot high-speed wind tunnel.

An appreciable margin was found between the critical Mach number and the Mach number at which an abrupt rise in drag coefficient occurred, and the supercritical drag rise was more abrupt for the nose inlets of higher critical Mach number.

Critical Mach numbers estimated from low-speed data were found to be conservative by a small amount when measured from a flat distribution and by a large amount when taken from sharp pressure peaks.

The formation of a negative pressure peak at the inlet lip generally resulted in an increase in drag over that associated with a flat pressure distribution. The Mach number at which the supercritical drag rise occurred was not appreciably affected by such pressure peaks and, therefore, by inlet-velocity ratio.

The supercritical drag rise for all three nose inlets was shown by wake profile and pressure distributions to result from a thickening of the boundary layer and from direct shock losses. A reduction of body fineness ratio from 8 to 5.5 by removal of a cylindrical section of the body led to no significant changes in the pressure drag; the decrease in drag measured was principally due to the change in wetted area of the body.

INTRODUCTION

Extensive low-speed wind-tunnel tests reported in references 1 and 2 furnish design data for the selection of a nose inlet or cowling which operates without adverse compressibility effects at the design high speed

of the airplane, and which fulfills the air-flow requirements of the power plant at the minimum value of the inlet-velocity ratio for which a pressure peak at the inlet lip is avoided. The high-speed design criterion used in these references is the nose-inlet critical Mach number, defined as the flight Mach number at which sonic velocity is first attained at some point on the nose inlet. Inasmuch as the reference tests were performed largely at low speeds, the values of critical Mach number were obtained by theoretical extrapolation of peak negative pressures. The Von Kármán theoretical variation of pressures with Mach number (reference 3) was used and was shown in reference 1 to be in good agreement with experiment for pressure distributions with no sharp local peaks.

The critical Mach number represents the upper limit of the Mach number range within which adverse changes in aerodynamic forces caused by compression shocks cannot occur. However, the critical Mach number can be exceeded by some increment before significant adverse changes in the aerodynamic forces occur, since the energy losses and pressure rise through a normal shock are zero at a local Mach number of 1.0 and at first increase slowly as the Mach number ahead of the shock is increased. This difference between the critical Mach number and the Mach number at which adverse compressibility effects arise has been observed in numerous airfoil investigations at supercritical speeds. Use of the critical Mach number criterion in the selection of a nose inlet or cowling is therefore conservative, since the selection will have a greater length and critical speed than actually required. Utilization of the shortest nose inlet possible may be desirable for reasons of airframe weight, ducting length, stability, pilot visibility, and lower minimum inlet-velocity ratio.

The investigation reported in this paper was undertaken for the purpose of studying the characteristics of NACA 1-series nose inlets at supercritical speeds with specific interest in the Mach number increment in excess of the critical speed for which the drag coefficient remains near subcritical values. The three nose inlets chosen for the tests represent a critical-speed cross section of the NACA 1-series nose inlets.

SYMBOLS

α angle of attack of nose-inlet center line, degrees

C_{D_e} external drag coefficient $\left(\frac{D_e}{q_o F}\right)$

c_d'	point drag coefficient
D_e	external drag, pounds
D	nose-inlet maximum diameter
F	nose-inlet frontal area, square feet
M	Mach number
P	pressure coefficient $\left(\frac{p - p_o}{q_o}\right)$
P_{max}	peak negative pressure coefficient
P_{cr}	critical pressure coefficient, corresponding to local Mach number of 1.0
p	static pressure, pounds per square foot
q	dynamic pressure, pounds per square foot $\left(\frac{1}{2}\rho V^2\right)$
r	radius, measured from nose-inlet center line
R	maximum nose-inlet radius (D/2)
ρ	air density, slugs per cubic foot
V	velocity, feet per second
x	axial distance from nose-inlet entrance

Subscripts

o	free stream
l	nose-inlet entrance
cr	critical
max	maximum

APPARATUS AND METHODS

The models were tested in the Langley 8-foot high-speed tunnel on a sting-strut support system schematically illustrated in figure 1(a). A photograph of the model installation is presented as figure 1(b). The model and strut cross-section areas were such as to permit the recording of valid test data with the tunnel choked, since the effective minimum area of the tunnel air stream occurred at the support strut. Accordingly, the highest Mach number of the tests was approximately 0.925.

The three NACA 1-series nose inlets of 3-inch maximum diameter tested (fig. 2) are designated after the method of reference 1 as the NACA 1-65-050, NACA 1-50-100, and NACA 1-40-200 nose inlets. The first number in the designation represents the series, the second group of numbers specifies the inlet diameter in percent of maximum diameter, and the third group of numbers specifies the nose-inlet length in percent of maximum diameter. Design critical Mach number and design (minimum) inlet-velocity ratio from reference 1 for each nose inlet are given in the following table:

NACA nose inlet	M_{cr}	$(V_1/V_o)_{min}$
1-65-050	0.700	0.18
1-50-100	.795	.20
1-40-200	.875	.40

Nose inlets of relatively low values of design inlet-velocity ratio were chosen for the investigation because of the limited flow which could be obtained with the ducting system.

Each nose inlet was mounted for tests on a common fuselage (fig. 2). The fuselage consisted of two parts: a removable cylindrical section, and an afterbody of NACA-111 proportions (reference 4) increased slightly in length. Each removable nose inlet was constructed with a cylindrical section of the length required to maintain an over-all model length identical for the three nose inlets. The complete model constituted a body of fineness ratio 8, in the range of current jet-fighter fuselage proportions. A fineness ratio of 5.5, corresponding to jet or turboprop nacelle proportions, was obtained by removing a portion of the cylindrical section of the fuselage.

As shown in figure 1(a), the internal flow was ducted through the sting and strut and into the test chamber. A throttle was used to regulate the mass flow, and a rake of static-pressure and total-pressure tubes in a venturi throat was used to measure the internal flow for calculation of the inlet-velocity ratio. The drag arising from the external flow over the body was measured by a wake-survey rake mounted on the sting a small distance aft of the sting-body juncture (fig. 1).

Pressure distributions over the exterior surfaces of each nose inlet and afterbody were measured by a row of pressure orifices on the upper surface in the vertical plane of symmetry.

Pressure-distribution measurements were made at angles of attack of 0°, 1.6°, and 3.7°. Drag measurements were made only at 0° angle of attack. The average variation of Reynolds number with Mach number in the 8-foot high-speed tunnel is given in figure 3.

RESULTS AND DISCUSSION

Pressure Distribution

Mach number.- Mach-number effects on the pressure distributions over the nose inlets and afterbodies for zero angle of attack are shown in figure 4 for the maximum inlet-velocity ratio permitted by the internal ducting system. Figure 5 gives the variation of the maximum obtainable inlet-velocity ratio with Mach number for each of the three nose inlets. The maximum values available at low Mach numbers for each inlet were greater than the design minimum inlet-velocity ratio and, consequently, high enough to provide the flat pressure-distribution characteristic of the 1-series nose inlets. For ease of reference, the nominal values of inlet-velocity ratio listed in figure 5 will be used to denote maximum inlet-velocity ratio.

The pressure distributions at low speeds show the favorable pressure-gradient characteristic of these nose inlets at values of inlet-velocity ratio greater than the design minimum value. The lowest pressure is near the nose inlet maximum diameter, beyond which the pressure rapidly increases to a value near the free-stream pressure along the cylindrical surface of the fuselage. The pressure again falls as the cylindrical surface terminates at the afterbody and finally increases to positive values near the sting-afterbody juncture. The shorter nose inlets have the higher peak pressures as would be expected from the lower design critical Mach numbers. As the Mach number is increased, the negative pressures tend uniformly to increase negatively until, when local sonic velocity is exceeded, a more pronounced pressure peak forms near the maximum diameter and the favorable low-speed pressure gradient steepens. Short horizontal marks on the curves indicate the critical pressure coefficient for the Mach number of the particular curve. The rearward movement of the pressure peaks of the NACA 1-65-050 and NACA 1-50-100 nose inlets (figs. 4(a) and 4(b)) with increasing Mach number in the supercritical range, and the steep pressure rise from these peaks signify the formation of a supersonic region terminated by a compression shock near the maximum diameter. A compression shock was probably present on the NACA 1-40-200 nose inlet at the highest Mach number of 0.924 (fig. 4(c)), but because of the relatively low induced velocities on this nose inlet, the losses through the shock are small.

For all three nose inlets, the absence of flow separation at supercritical Mach numbers is indicated in the maintenance of good pressure recovery at the tail of the body for the entire range of Mach number.

Inlet-velocity ratio.- It has often been assumed, in the absence of high-speed data to the contrary, that the presence of sharp pressure peaks indicated that adverse compressibility effects would occur if the corresponding critical Mach number was exceeded. This effect was assumed in setting up the design procedures of references 1 and 2, in that the inlet-velocity ratio is specified sufficiently high to preclude pressure peaks at the inlet lip.

Important qualifications to this assumed condition have been found in the present tests. Figures 6, 7, and 8 show pressure distributions for several values of inlet-velocity ratio at subcritical and supercritical Mach numbers for the three nose inlets. At the subcritical Mach numbers, a pressure peak is shown at the inlet lip for each configuration at zero inlet velocity (figs. 6(a), 7(a), and 8(a)). At supercritical Mach numbers (figs. 6(b), 7(b), and 8(b)), the pressure peak at the lip disappeared on the NACA 1-65-050 and NACA 1-50-100 nose inlets. The minimum pressure occurred near the maximum diameter, and was affected very little by inlet-velocity ratio. For the NACA 1-40-200 nose inlet, however, the pressure peak remained at the inlet lip for zero inlet-velocity ratio. Although the orifice spacing does not permit a conclusive observation, it appears likely that an immediate compression from this peak to pressures corresponding to subsonic velocity did not occur.

Clearly, for the NACA 1-65-050 and NACA 1-50-100 nose inlets, inlet-velocity ratio does not exert the important influence on the shock losses and drag at supercritical speeds which had been predicted from low-speed studies. A larger effect of inlet-velocity ratio on the drag of the NACA 1-40-200 nose inlet at supercritical speeds is inferred from the pressure distributions, since a considerable effect of inlet-velocity ratio on the induced velocities near the lip of this nose inlet was measured (fig. 8(b)). Again, however, the pressure minimum before the shock near the nose-inlet maximum diameter was relatively insensitive to inlet-velocity ratio.

The variation of peak negative pressures with Mach number for the three nose inlets is given in figure 9 for zero and maximum inlet-velocity ratio. The Von Kármán theoretical variation of pressure coefficient is plotted from the pressure coefficients at a Mach number of 0.4. The peak negative pressures of the NACA 1-65-050 and NACA 1-50-100 nose inlets at zero inlet-velocity ratio were measured at the inlet lip at low Mach numbers, and near maximum diameter at higher Mach numbers, while the peak pressure at zero inlet-velocity ratio for the NACA 1-40-200 nose inlet remained at the lip throughout the Mach number range. The flagged symbols in figure 9(b) give the values of the local pressure peak near

maximum diameter for those Mach numbers at which pressure peaks both at the lip and near maximum diameter were recorded. Because of the short length of the NACA 1-65-050 nose inlet, no second pressure peak near maximum diameter at the lower Mach numbers was observed for this nose inlet at zero inlet-velocity ratio (fig. 6(a)).

The effect of inlet-velocity ratio on the peak negative pressure of the NACA 1-65-050 and NACA 1-50-100 nose inlets is shown to be small near and above the critical Mach number. For blunt nose inlets such as these, therefore, considerable error can exist in the estimation of critical Mach number from low-speed tests for the low inlet-velocity-ratio range wherein a pressure peak exists at the lip. As indicated by the flagged symbols of figure 9(b), a more accurate estimate of the critical Mach number can be made under these circumstances by extrapolating the low-speed pressure peak near the nose-inlet maximum diameter, rather than the sharper (and more negative) peak at the lip.

The variation of peak pressures with Mach number for the NACA 1-40-200 nose inlet are shown in figure 9(c) to be similar for the two inlet-velocity ratios shown. In constrast with the results shown for the blunter nose inlets of the tests, the effect of inlet-velocity ratio upon critical Mach number for this nose inlet is large, which is apparently a result of the relatively thin lip of the NACA 1-40-200 nose inlet.

Angle of attack.- Pressure distributions at two positive angles of attack are shown for the NACA 1-50-100 nose inlet in figures 10 and 11. A comparison of these curves with those of figure 7 indicates that the effect of positive angle of attack on pressure distribution on the upper surface is a small increase of pressures on the cylindrical midsection and afterbody with a slight decrease of pressures at, and forward of, the maximum nose-inlet diameter. In contrast with the pressure distribution at zero angle of attack, a pressure peak at the inlet lip is found to persist into supercritical speeds for low inlet-velocity ratio. While the slightly lower pressure just before the shock of the nose inlet at an angle of attack increases the pressure rise and energy loss through the shock, the absence of separation is indicated by the magnitude of the pressure recovery at the end of the body for 3.7° angle of attack (fig. 11(b)).

Fineness ratio.- In figures 12, 13, and 14, a comparison of the subcritical and supercritical pressure distributions is given for two fineness ratios. The low fineness ratio (5.5) was obtained by removing a cylindrical center section 2.5 diameters in length (fig. 2). The low-fineness-ratio fuselage retained a cylindrical center section as shown in the figure, which was of greatest length for the shortest nose inlet (NACA 1-65-050). Little change in the pressure distribution over the nose inlets resulted from the change of fineness ratio. Furthermore, the pressure recovery at the tail of the fuselage and the minimum pressure

before the shock were affected very little by the change of fineness ratio. Hence, the drag may be expected to differ only by the skin-friction difference for the two fineness ratios.

Drag

The variation of drag coefficient with Mach number for the three nose inlets tested is presented in figure 15 for inlet-velocity ratios of zero and the maximum available. Also, the drag for a constant inlet-velocity ratio of 0.2 is shown for the NACA 1-40-200 nose inlet. The external drags of the NACA 1-50-100 and NACA 1-65-050 nose inlets were affected very little by inlet-velocity ratio over the Mach number range. For the NACA 1-40-200 nose inlet, little change occurred when the inlet-velocity ratio was decreased from 0.5 to 0.2; however, when the inlet-velocity ratio was further decreased to zero, at which point a pressure peak has been shown to exist through the Mach number range, a significant drag increase resulted.

A comparison of the drag characteristics of the three nose inlets is given in figure 16 for the maximum inlet-velocity ratio of the tests. The short vertical marks on the curves denote the critical Mach numbers predicted by the selection chart of reference 1, and the arrows identify the actual critical Mach numbers read from figure 9. The predicted critical Mach numbers are seen to be conservative by a small amount (approximately 0.015 to 0.025). An appreciable margin exists, particularly for the NACA 1-65-050 and NACA 1-50-100 nose inlets, between the critical Mach number and the Mach number at which a significant drag rise occurs.

A steeper drag rise was found for the nose inlets of higher design critical Mach number. As discussed in reference 5, this characteristic of the supercritical drag rise is associated with the body contour in the region of the shock; the nose inlets of higher critical speed have more gradually faired contours with a larger radius of curvature at the position of the compression shock (near the maximum diameter of the nose inlet); the velocity gradient normal to the surface at the shock is therefore smaller, and consequently, for a given velocity at the surface, the induced superstream velocity extends further from the nose-inlet surface. While a specified increment of Mach number above the critical does not exactly correspond to a specified local supersonic velocity, the effects of the difference are minor compared with the effects of the body contour, and, therefore, for a specified increment of Mach number above the critical, the extent of the shock and the total shock losses are greater for the nose inlets of higher critical speed.

Wake profiles given in figure 17 for the maximum inlet-velocity ratio of the tests illustrate the character of the losses and the changes

which occur with Mach number. The radial variation of point drag coefficient is given for the lowest test Mach number, a Mach number near the critical, and the highest test Mach number. The point drag coefficient is a measure of the elemental drag arising from the local momentum defect at that point (reference 6). A gradual decrease of drag coefficient with Mach number is shown in figure 16 for each nose inlet up to the critical Mach number. Accordingly, in the wake profiles of figure 17, boundary-layer losses smaller than those at the lowest Mach number are observed for the Mach numbers near critical. This reduction in drag coefficient is believed to result from the decrease of the skin-friction coefficient with the increase of Reynolds number. The NACA 1-65-050 and NACA 1-50-100 nose inlets exhibit an extensive shock loss at the highest Mach number, while only a very small shock loss is evident for the NACA 1-40-200 nose inlet. This small shock loss and an increase of boundary-layer losses over those for the critical Mach number together comprise the supercritical drag rise shown for the NACA 1-40-200 nose inlet in figure 16.

The significance of a sharp pressure peak on a nose-inlet lip at supercritical speeds may be evaluated by reference to the supercritical characteristics of the NACA 1-40-200 nose inlet. In figure 9(c), it was shown that, for the NACA 1-40-200 nose inlet, the reduction of inlet-velocity ratio to zero effected appreciable change in the critical Mach number, since the pressure peak raised at the nose-inlet lip at zero inlet-velocity ratio persisted to supercritical speeds. The critical Mach number was reduced from 0.89 for the maximum inlet-velocity ratio to 0.807 for zero inlet-velocity ratio. This peak at the lip led to an increase of drag at all Mach numbers over the drag for a flat pressure distribution because of the increased skin friction, but no supercritical drag rise was measured (fig. 15(c)) at zero inlet-velocity ratio when the critical Mach number was exceeded by the large margin of 0.11.

The phenomenon just discussed is evidently more concerned with the boundary layer than with shock or shock effects. At high values of inlet-velocity ratio, the increase in drag of the NACA 1-40-200 nose inlet which occurs at $M = 0.924$ is seen by reference to figure 17(c) to result principally from increased losses in the boundary layer. In view of the low drag and the small adverse pressure gradient aft of the nose of this body, it appears likely that considerable laminar flow existed at low Mach numbers. At the maximum test Mach number, the steepened gradient which followed the region of local supersonic flow on the nose inlet (fig. 8) evidently moved transition forward, thus increasing the drag. On the other hand, the existence of a sharp pressure peak at the lip of this nose inlet at zero inlet-velocity ratio at all Mach numbers indicates that transition occurred well forward in the Mach number range when the inlet-velocity ratio was zero. Hence, the transition shift and associated drag increase which occurred for the high inlet-velocity-ratio condition did not take place. Further, inasmuch as essentially

identical shock losses occur (fig. 18) for both inlet-velocity ratios at the highest Mach number and inasmuch as the pressure before the shock is identical for these two cases (fig. 8), a similar rate of drag rise might be expected for the two inlet-velocity ratios at Mach numbers above the highest obtained in the present tests.

A comparison of the drag characteristics of the nose inlets in conjunction with bodies of two fineness ratios is shown in figure 19. Drag data at Mach numbers only up to approximately the respective criticals were obtained with the low-fineness-ratio bodies because a rake of length adequate to measure shock losses (used for the high-fineness-ratio tests) was not available at that time. The drag increment shown between the two fineness ratios is approximately that which would be expected from the change of wetted area involved. The decrease of drag coefficient with Mach number is observed to be less for the low-fineness-ratio body than for the high-fineness-ratio body.

The increase in the drag coefficient of the NACA 1-40-200 low-fineness-ratio body as the Mach number was increased from 0.6 to 0.75 is presumed to be a result of the concomitant increase of Reynolds number. Figure 20 gives the pressure distributions for Mach numbers in the range of the drag increase and indicates that changes in pressure distribution are not sufficiently large to produce an increase of pressure drag or a change in the position of the transition point. The Reynolds number change associated with the Mach number increase, however, may possibly have moved the transition point forward from some point A (fig. 21) to some point B. Because of the more adverse pressure gradient of the high-fineness-ratio body near the nose-inlet maximum diameter, the transition point was probably at some more forward position C, and was less sensitive to Reynolds number than the transition point of the low-fineness-ratio body. (As discussed previously in the section entitled "Drag," from point C the transition point was subsequently moved forward by the shock which formed near maximum diameter at a Mach number of 0.924.)

DESIGN CONSIDERATIONS

It is desirable to consider the application of the results of the present investigation to the design of nose inlets, in particular to the design procedures set forth in references 1 and 2.

On the basis of predicting the supercritical drag rise, critical Mach number has been shown to be conservative (fig. 16) in some cases by a considerable margin. It follows, therefore, that a nose inlet may be selected for a critical Mach number somewhat lower than the design flight value with assurance of freedom from adverse compressibility effects. If, in so doing, the fuselage or body can be made shorter, a reduction in drag may result (fig. 19) due simply to the reduction in wetted area.

In cases where the body length is fixed by other considerations, however, the lower induced velocities over the nose inlets of higher critical Mach number make desirable the use of a nose inlet of as high a critical Mach number as possible. For example, figure 16 shows that a body with the NACA 1-40-200 nose inlet has, at subcritical speeds, a drag only 75 percent of that of the body (of the same over-all length) with an NACA 1-65-050 nose inlet.

The flat pressure-distribution characteristic of the NACA 1-series nose inlets is shown to permit attainment of relatively low values of fuselage drag coefficient (fig. 16) by virtue of low induced velocities and a pressure gradient over the nose inlet favorable to the formation of a relatively extensive laminar boundary layer. The change in the drag caused by the formation of a pressure peak at the inlet lip was generally found to be detrimental, although in one case (the NACA 1-50-100 nose inlet at Mach numbers above 0.6, fig. 15(b)), the increase of drag was immeasurably small. The results of the NACA 1-40-200 nose-inlet measurements lead to the conclusion that a pressure peak which is formed at low-inlet-velocity ratios at the inlet lip, and which persists into supercritical speeds, may not affect the Mach number of the supercritical drag rise, although the pressure peak may substantially reduce the critical Mach number. Furthermore, little effect of such a pressure peak on the characteristics of the supercritical drag rise should be expected inasmuch as identical shock losses and identical pressures ahead of shock were found (figs. 8 and 18). These results thus demonstrate that the flat pressure distribution offers a definite advantage at Mach numbers extending into the supercritical range.

CONCLUSIONS

The principal conclusions drawn from a study of the characteristics of three NACA 1-series nose inlets at Mach numbers up to 0.925 follow:

1. An appreciable margin existed between the critical Mach number and the Mach number at which an abrupt rise in drag coefficient occurred. The supercritical drag rise was more abrupt for the nose inlets of higher crtical Mach number.

2. The negative pressure peak which occurs on the nose-inlet lip at low-inlet-velocity ratios (below the design value) tends to disappear at high Mach numbers for the blunter nose inlets, while continuing to exist for the inlets with sharper lips. Consequently, critical Mach numbers estimated from these peaks at low speeds may be conservative by a large amount. Critical Mach numbers estimated from the normal (flat) pressure distribution or from the pressure minimum near the nose-inlet maximum diameter were found to be conservative by a small amount.

3. The formation of a negative pressure peak at the inlet lip generally resulted in an increase in drag over that associated with a flat pressure distribution. This increase was minor for the NACA 1-65-050 and NACA 1-50-100 nose inlets but appreciable for the NACA 1-40-200 nose inlet.

4. The Mach number at which the supercritical drag rise occurred was not appreciably affected by sharp peaks at the lip, and, therefore, by inlet-velocity ratio.

5. The supercritical drag rise for all three nose inlets was shown by wake profiles and pressure distributions to be due to a thickening of the boundary layer and to direct shock losses, rather than to shock-induced separation.

6. A reduction of body fineness ratio from 8 to 5.5 (by removal of a portion of the cylindrical section of the body) led to no significant changes in the pressure drag. The decrease in drag measured was principally due to the change in wetted area of the body.

Langley Aeronautical Laboratory
National Advisory Committee for Aeronautics
Langley Field, Va.

REFERENCES

1. Baals, Donald D., Smith, Norman F., and Wright, John B.: The Development and Application of High-Critical-Speed Nose Inlets. NACA ACR No. L5F30a, 1945.

2. Nichols, Mark R., and Keith, Arvid L., Jr.: Investigation of a Systematic Group of NACA 1-Series Cowlings with and without Spinners. NACA RM No. L8A15, 1948.

3. Von Kármán, Th.: Compressibility Effects in Aerodynamics. Jour. Aero. Sci., vol. 8, no. 9, July 1941, pp. 337-356.

4. Abbott, Ira H.: Fuselage-Drag Tests in the Variable-Density Wind Tunnel: Streamline Bodies of Revolution, Fineness Ratio of 5. NACA TN No. 614, 1937.

5. Zobel, Th.: Results on Tests on Various Axially Symmetrical Radiator Cowlings. Reps. and Translations No. 365, British M.O.S. (A.B.) Völkenrode, Jan. 1946.

6. Baals, Donald D., and Mourhess, Mary J.: Numerical Evaluation of the Wake-Survey Equations for Subsonic Flow Including the Effect of Energy Addition. NACA ARR No. L5H27, 1945.

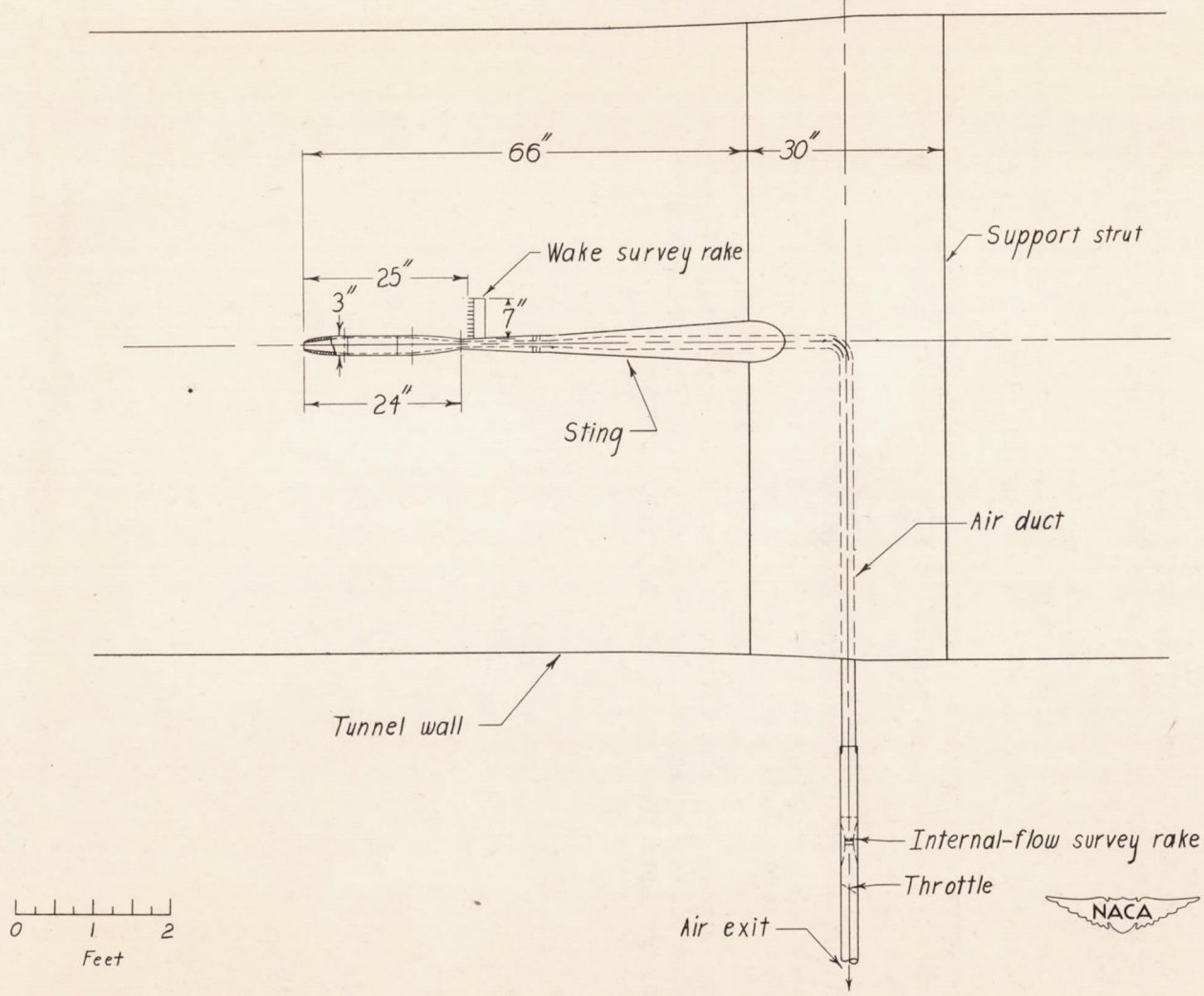

(a) Model installation and details.

Figure 1.- Experimental setup.

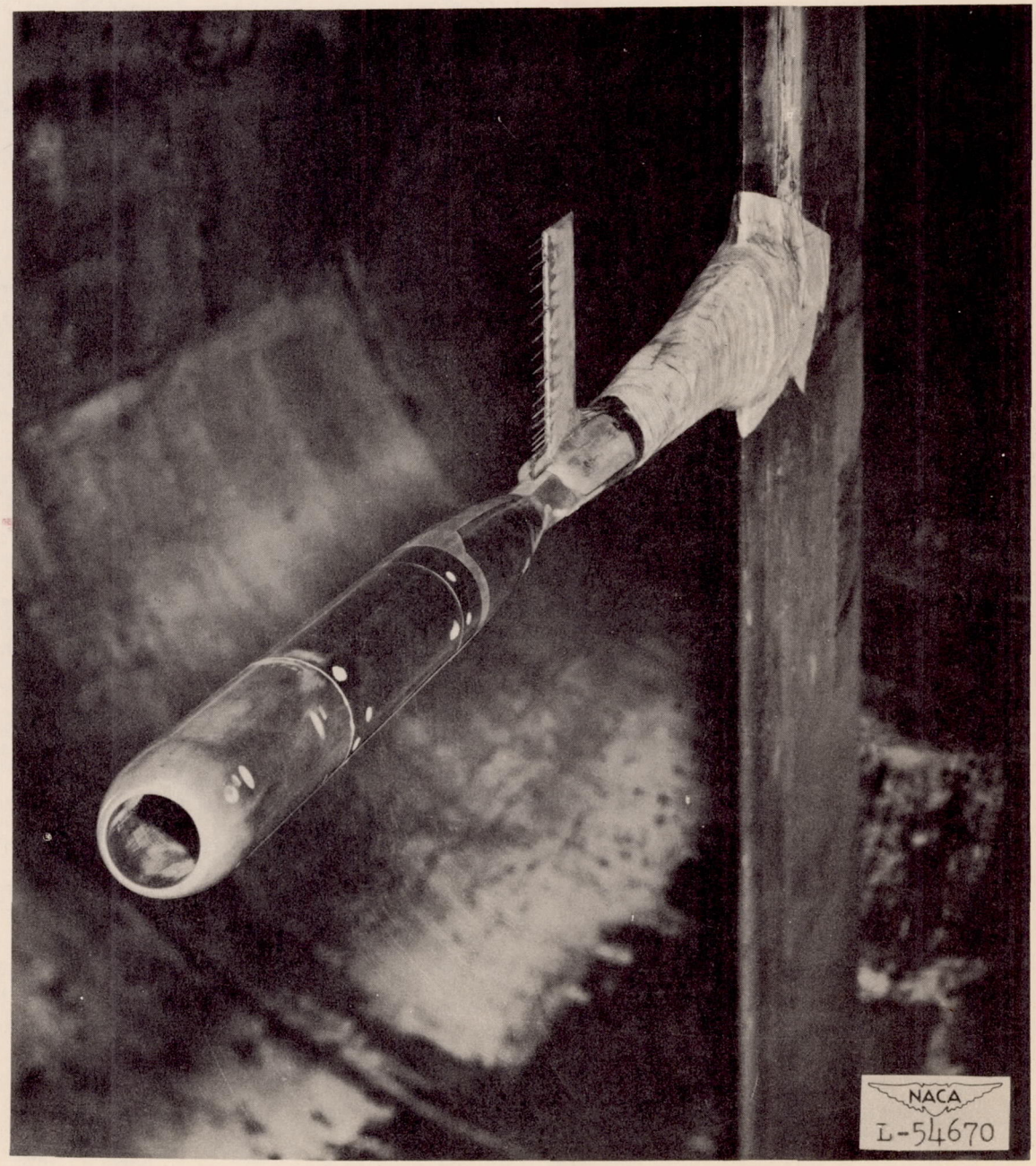

(b) Photograph of model and wake—survey rake installation.

Figure 1.— Concluded.

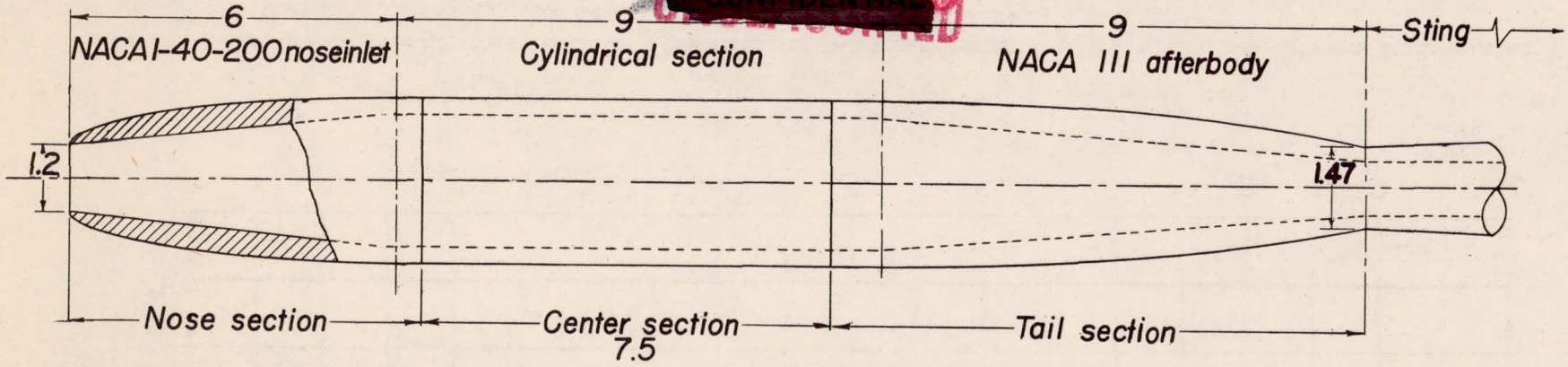

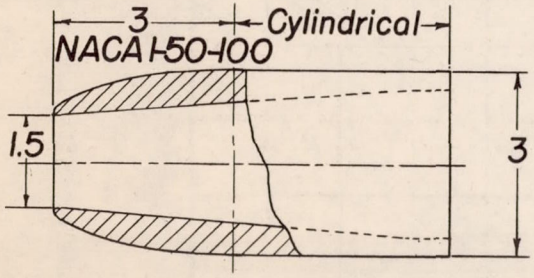

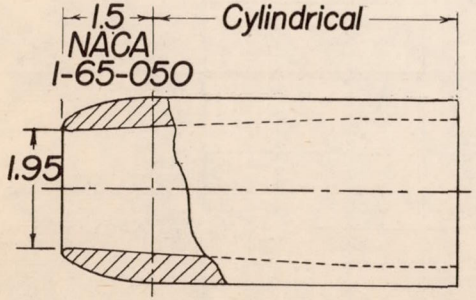

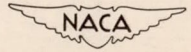

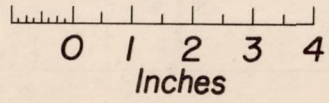

Figure 2.– Fuselage configuration and nose inlets tested.

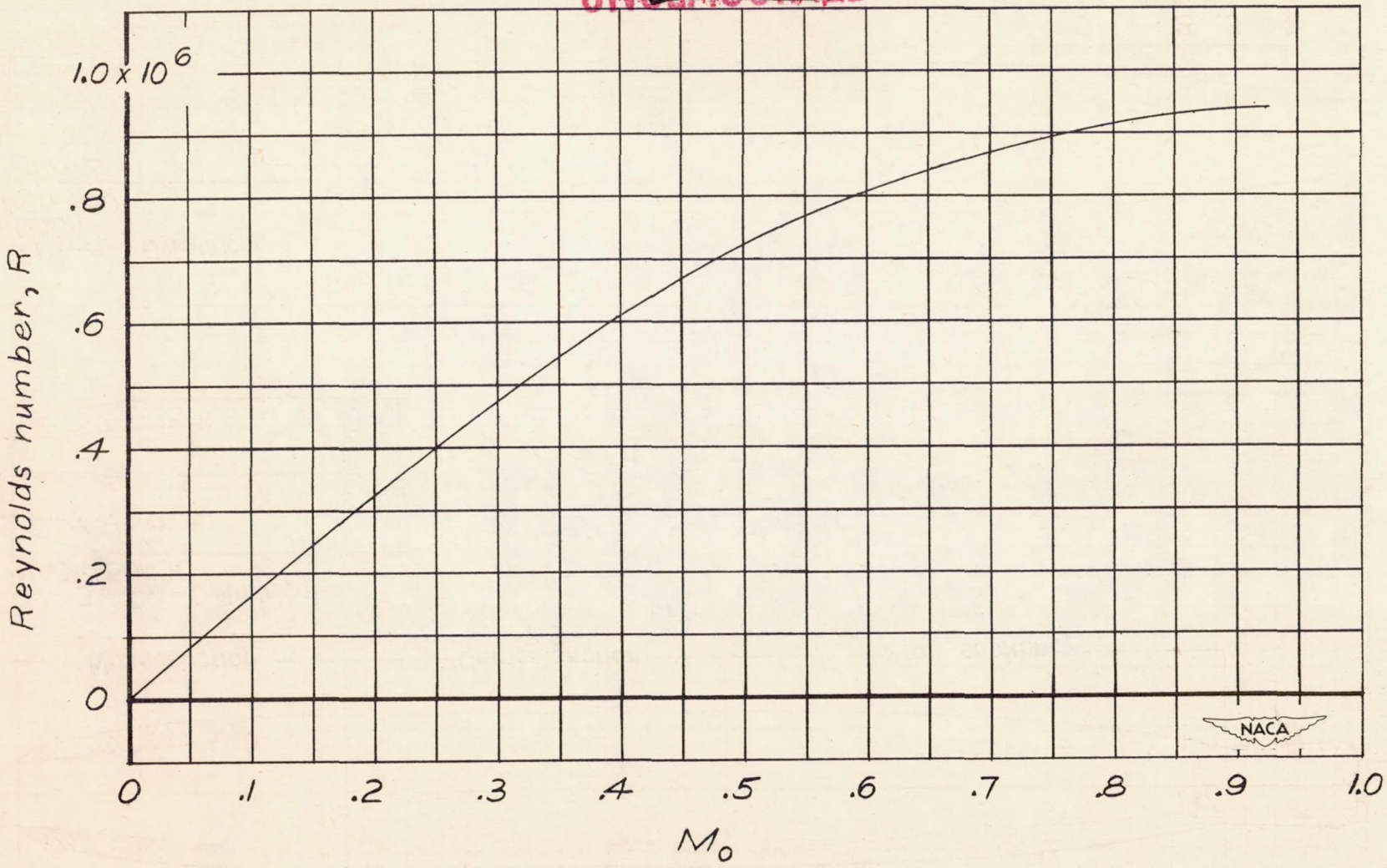

Figure 3.- Variation of Reynolds number (based on a 3-inch-diameter body) with free-stream Mach number in Langley 8-foot high-speed tunnel.

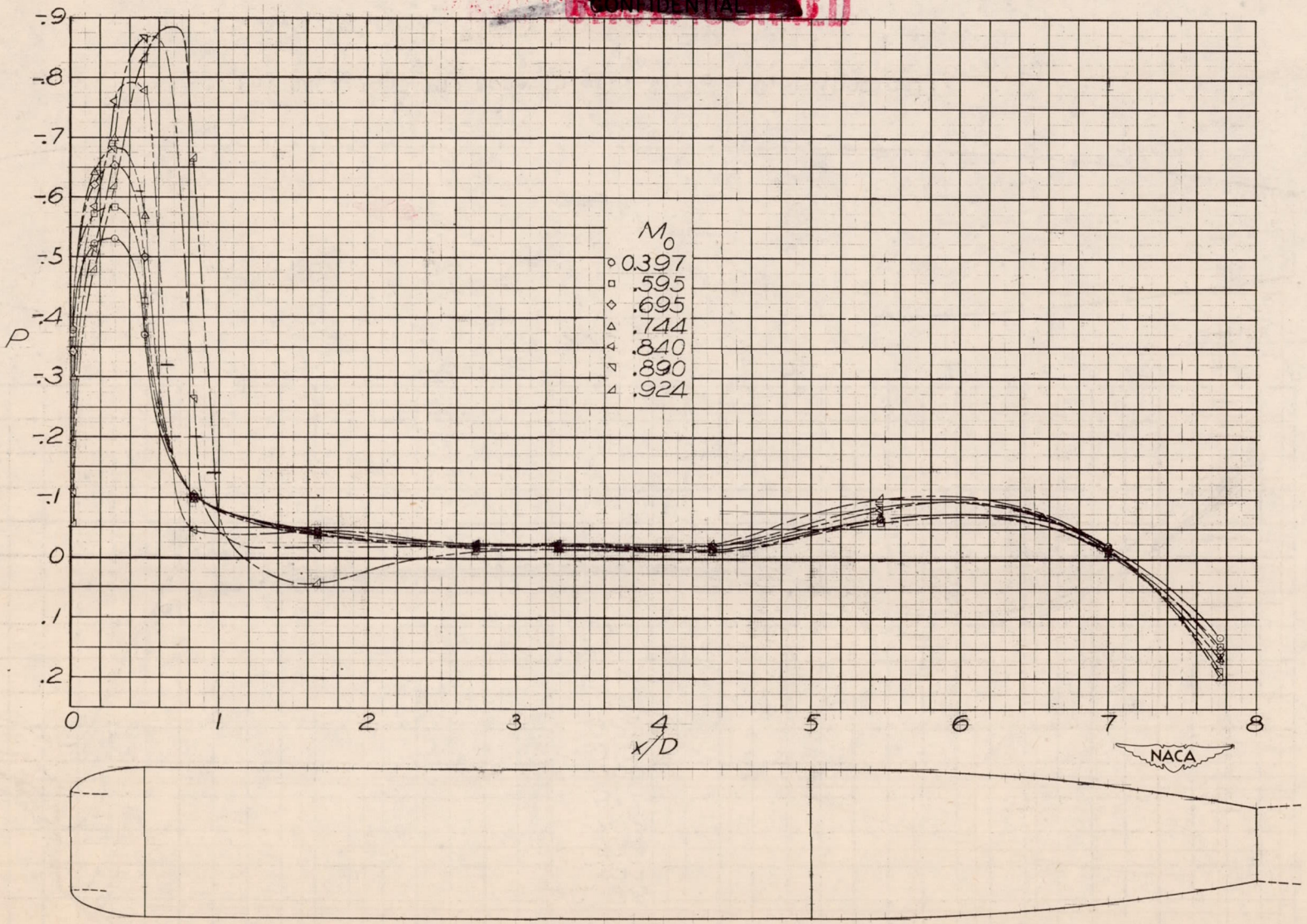

(a) NACA 1-65-050 nose inlet. V_1/V_o = 0.18 (nominal).

Figure 4.- Mach number effects on pressure distribution. $\alpha = 0^o$.

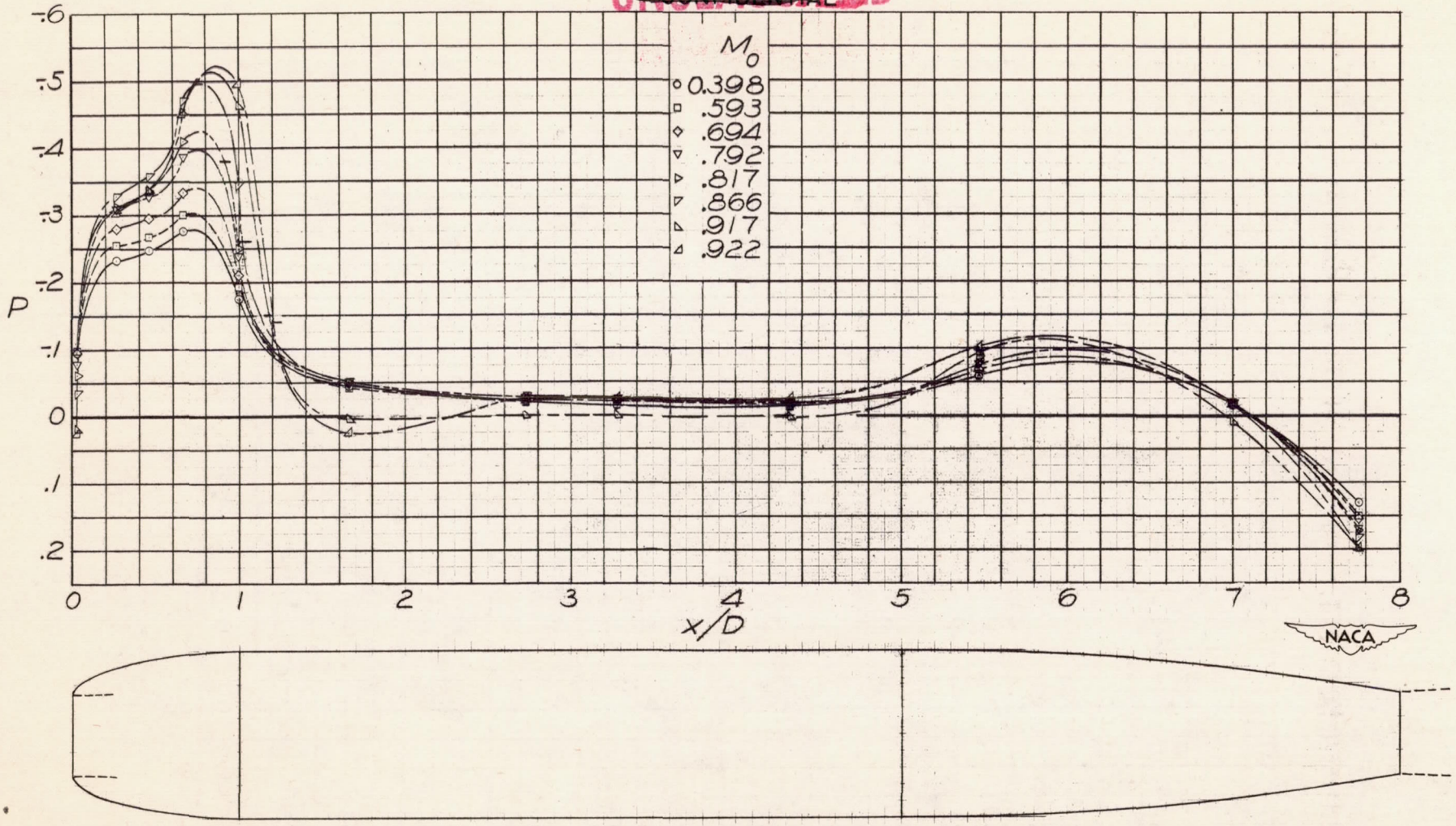

(b) NACA 1-50-100 nose inlet. V_1/V_o = 0.3 (nominal).

Figure 4.- Continued.

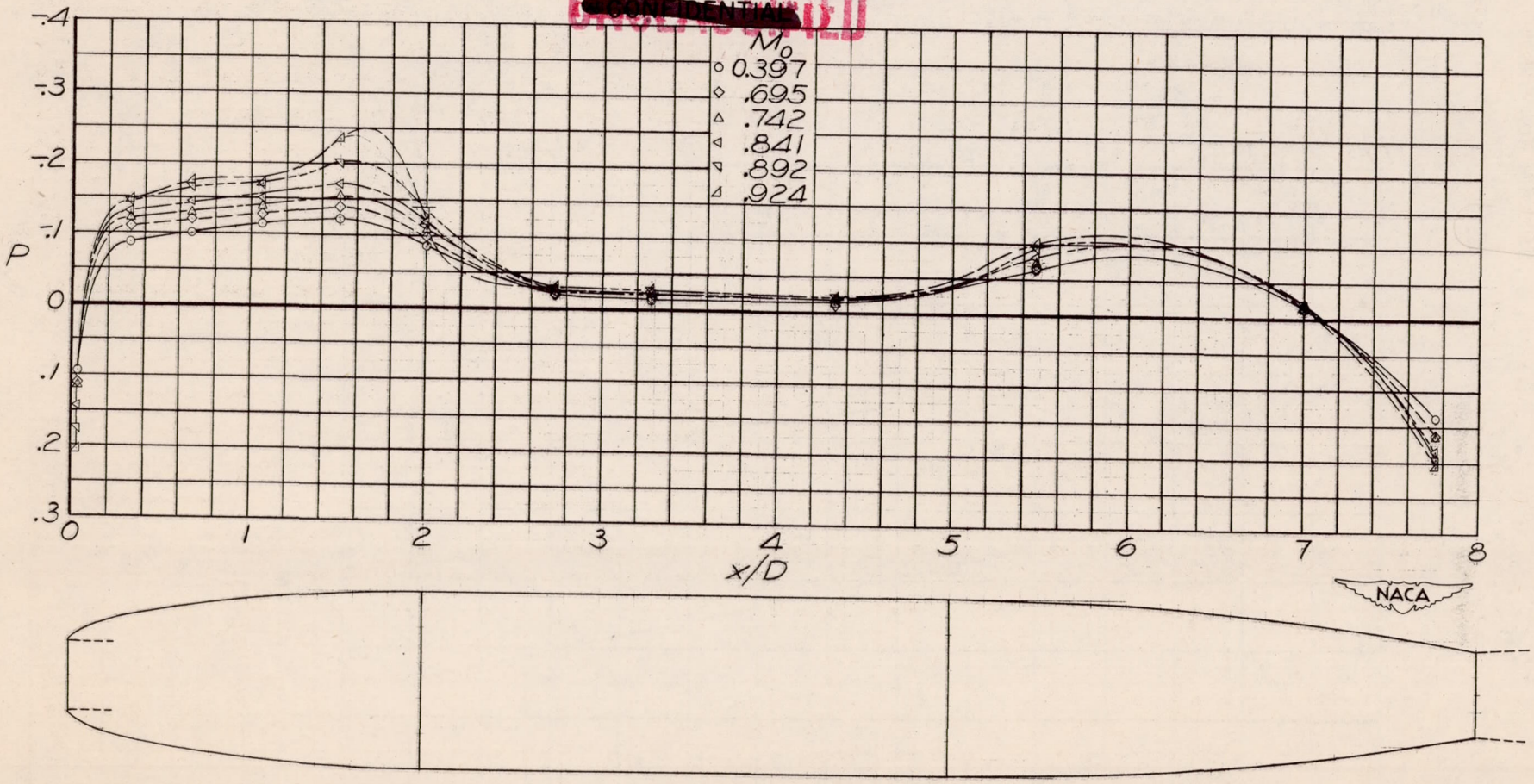

(c) NACA 1-40-200 nose inlet. $V_1/V_o = 0.5$ (nominal).

Figure 4.- Concluded.

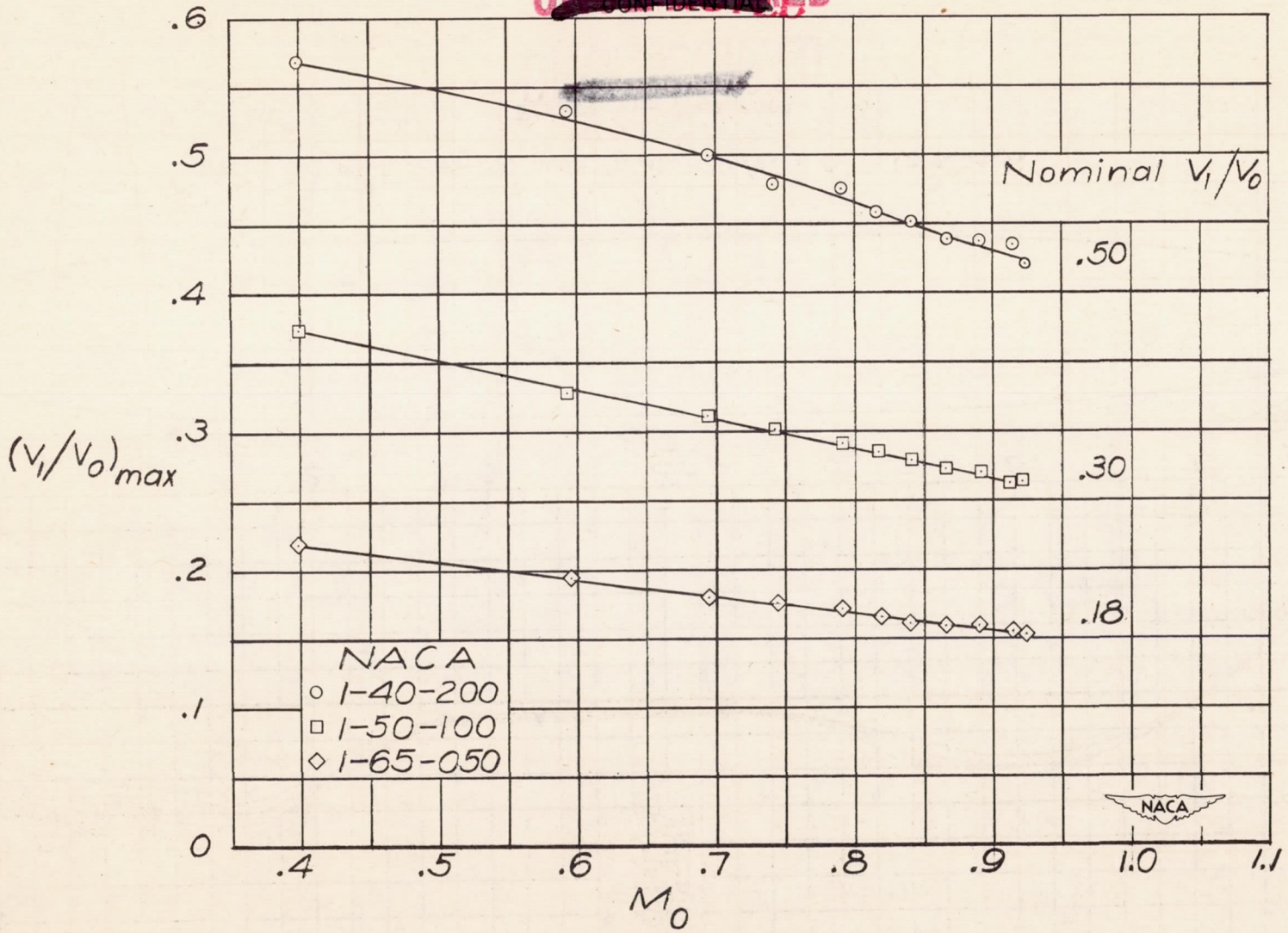

Figure 5.- Variation of maximum available inlet-velocity ratio with Mach number.

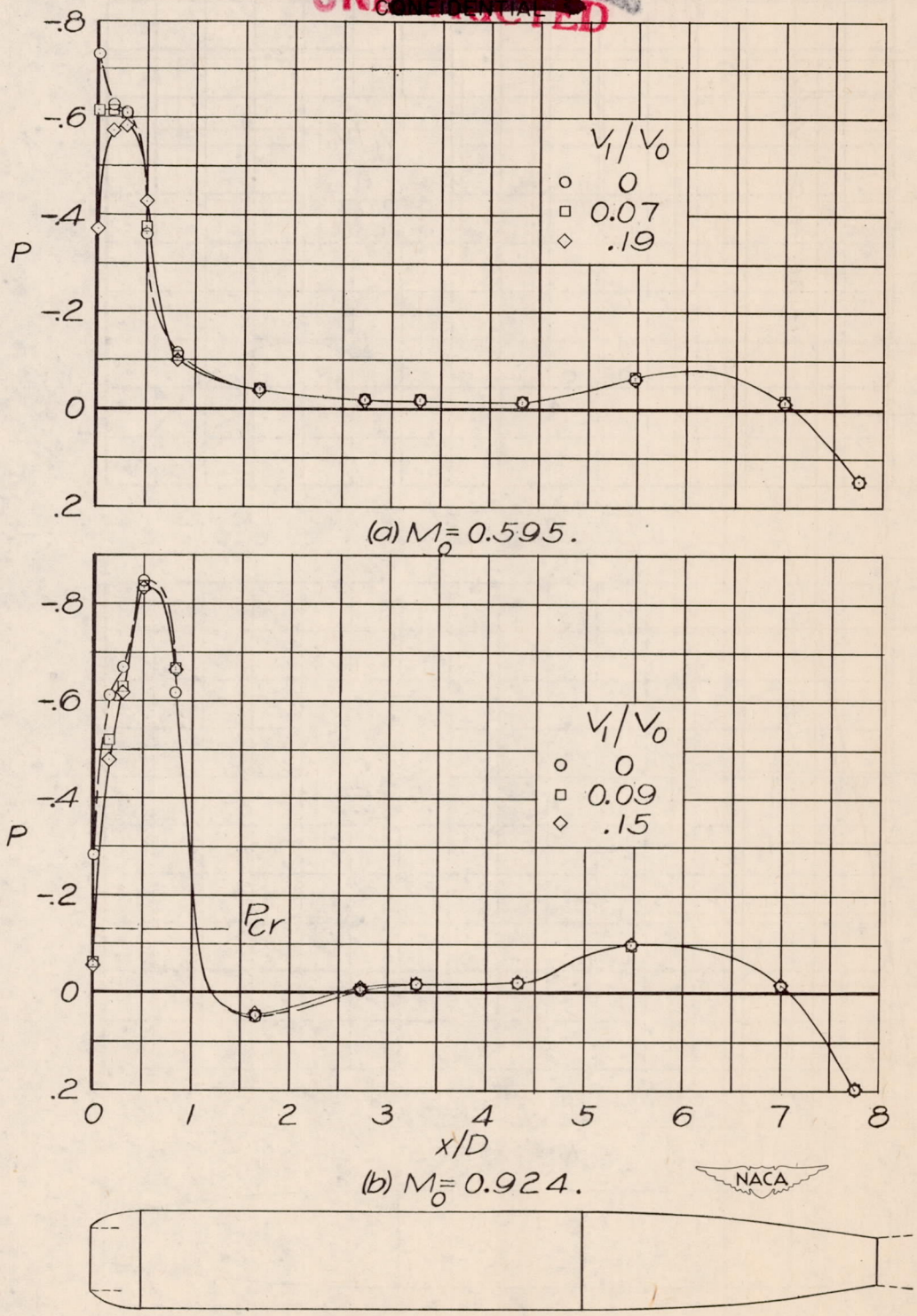

Figure 6.– Effect of inlet–velocity ratio on pressure distribution at subcritical and supercritical Mach numbers. NACA 1–65–050 nose inlet; $\alpha = 0^\circ$.

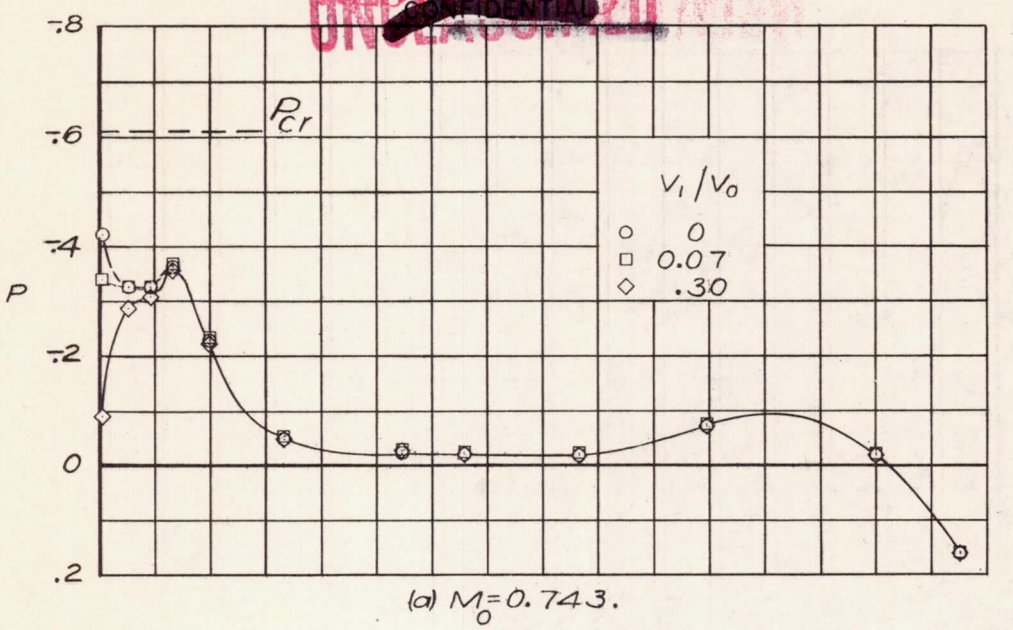

(a) $M_0 = 0.743$.

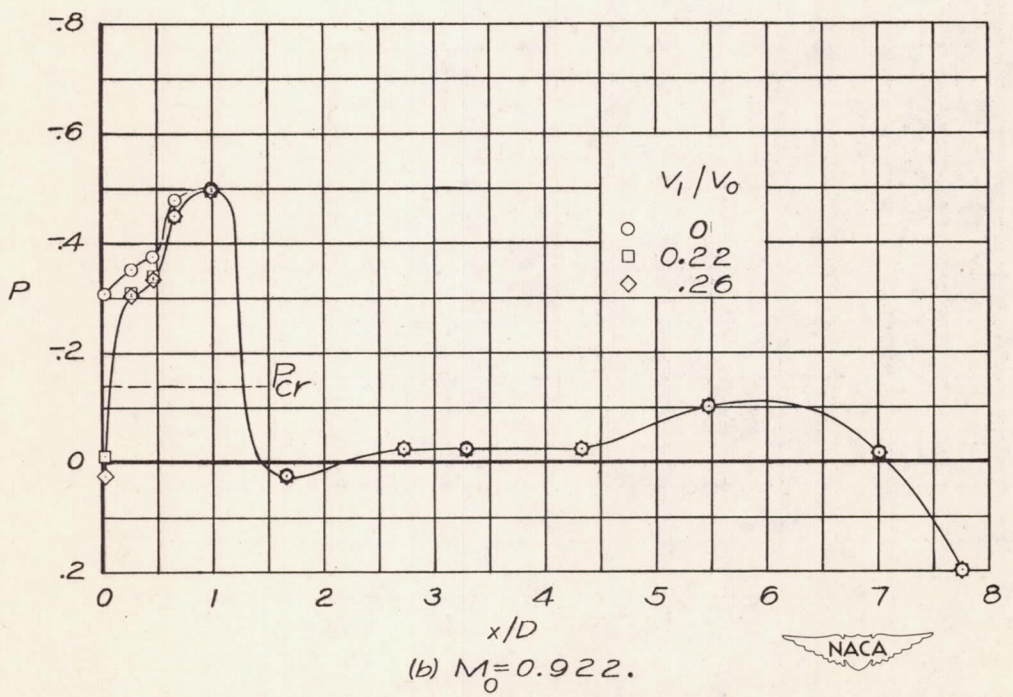

(b) $M_0 = 0.922$.

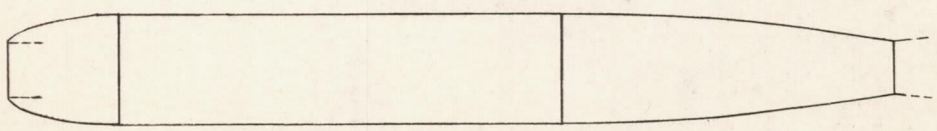

Figure 7.– Effect of inlet–velocity ratio on pressure distribution at subcritical and supercritical Mach numbers. NACA 1–50–100 nose inlet; $\alpha = 0^\circ$.

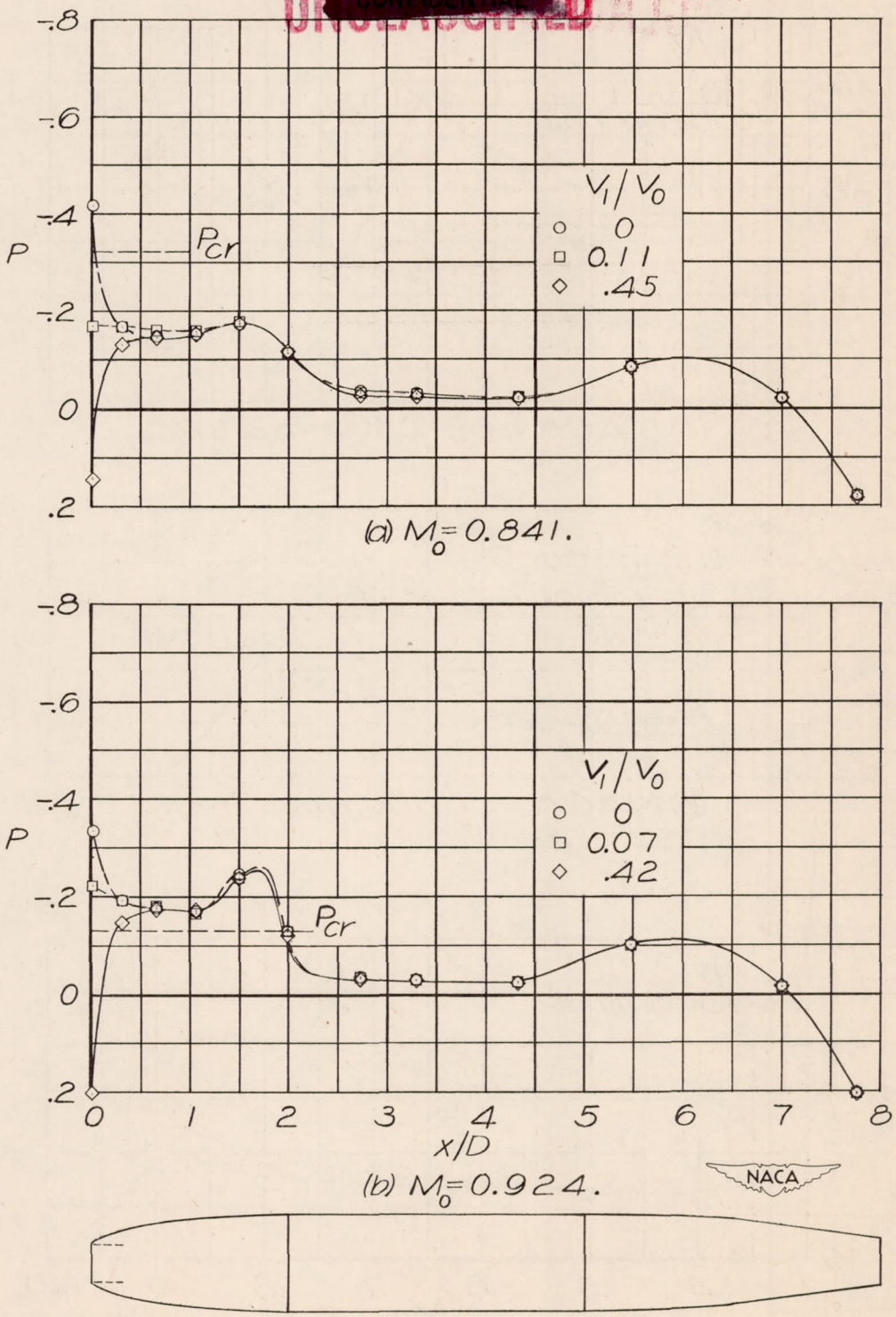

Figure 8.– Effect of inlet–velocity ratio on pressure distribution at subcritical and supercritical Mach numbers. NACA 1–40–200 nose inlet; $\alpha = 0^\circ$.

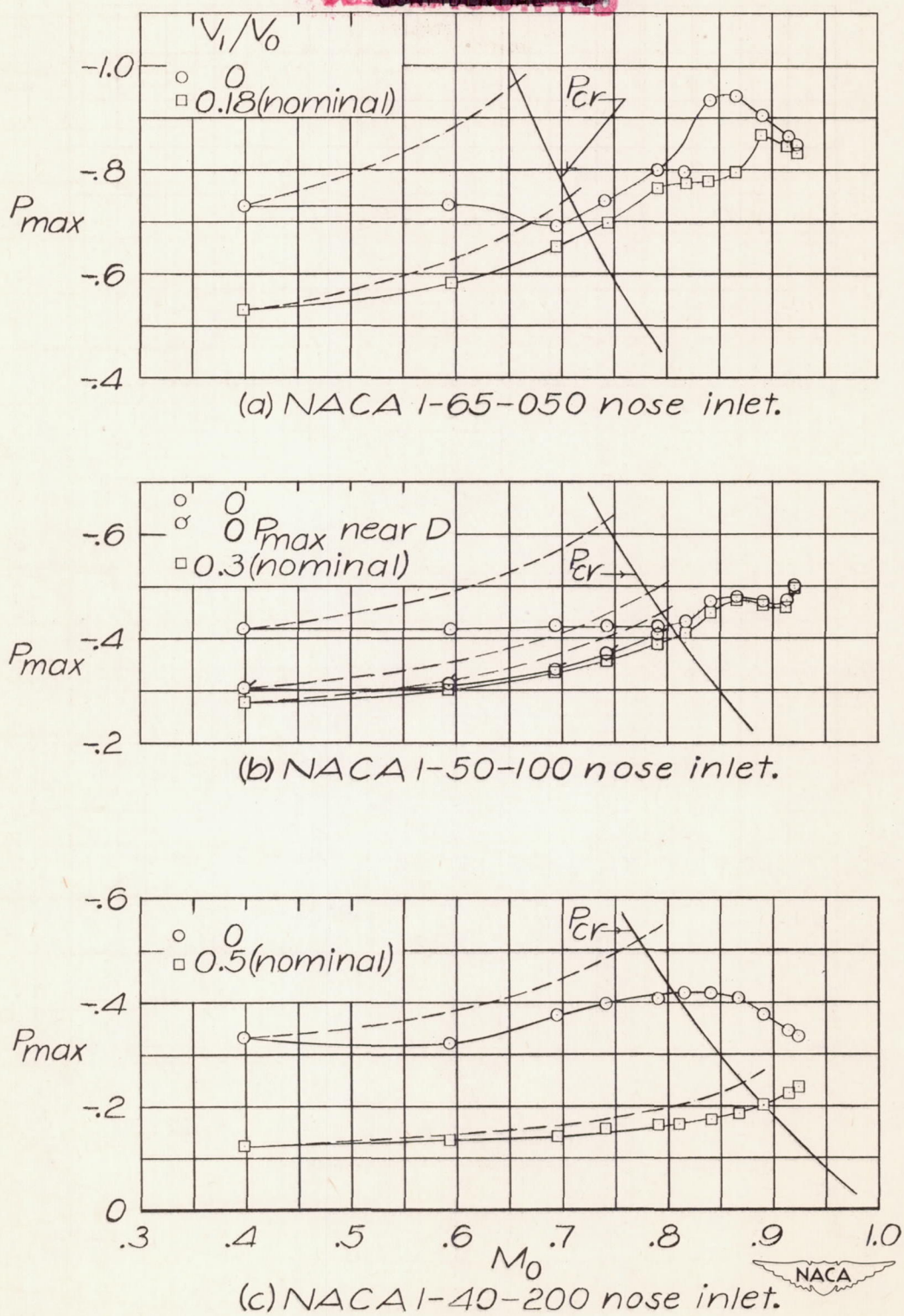

Figure 9.– Compressibility effect on peak negative pressure coefficient. $\alpha = 0^\circ$. Dashed curves give the theoretical variation (reference 3).

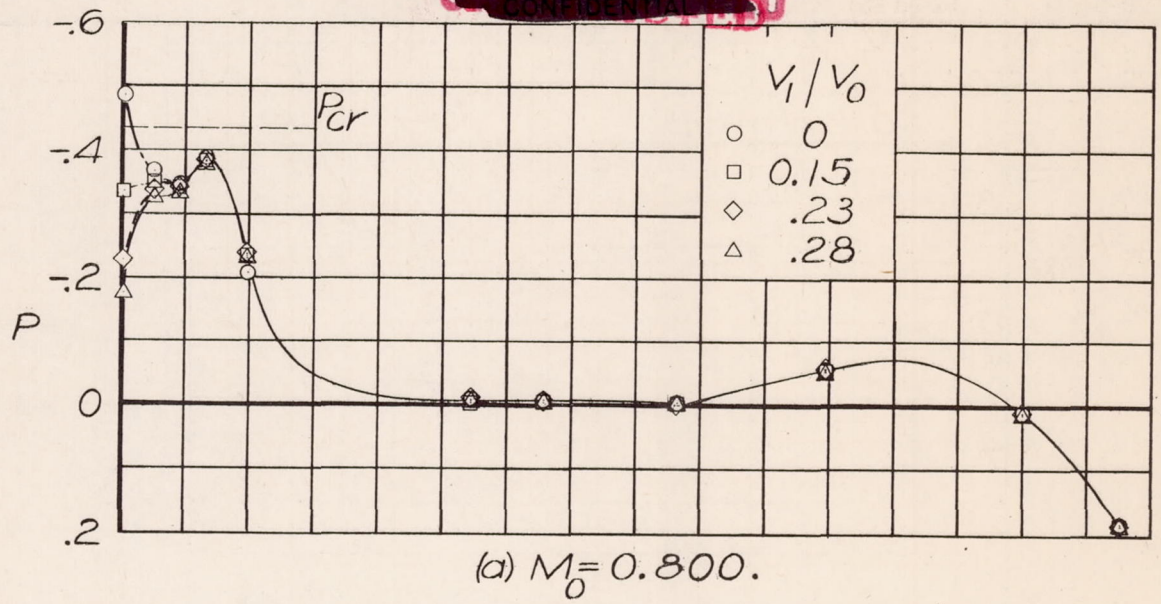

(a) $M_0 = 0.800$.

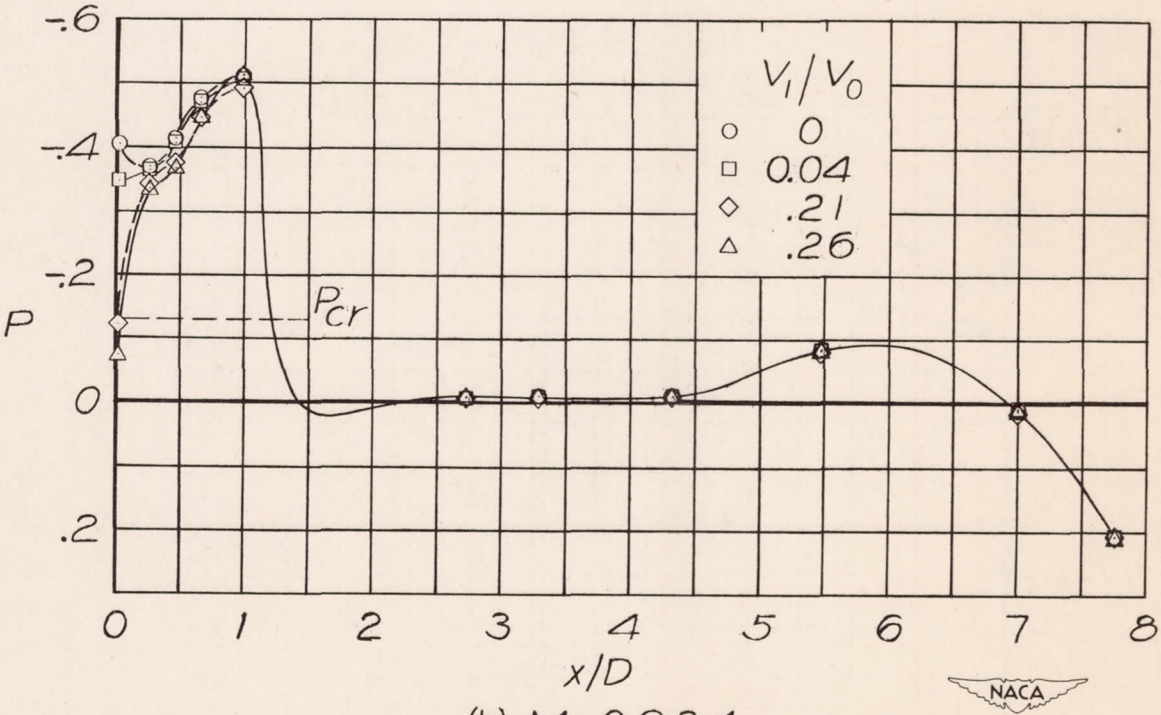

(b) $M_0 = 0.924$.

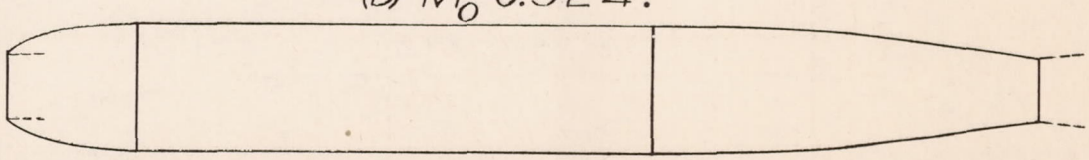

Figure 10.– Pressure distribution on NACA 1–50–100 nose inlet; $\alpha = 1.6°$.

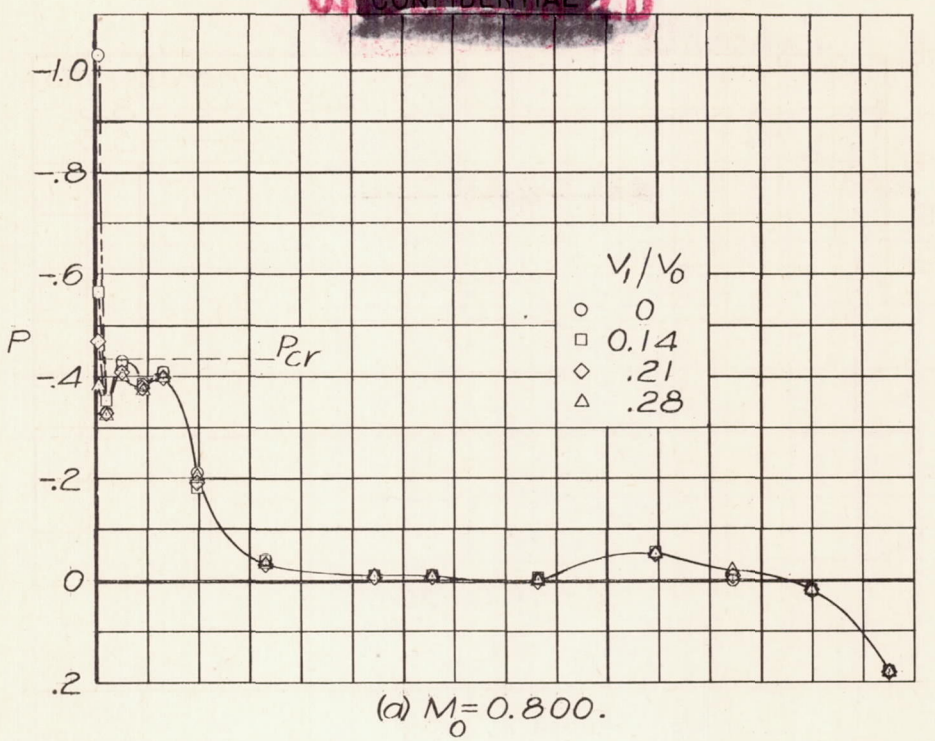

(a) $M_0 = 0.800$.

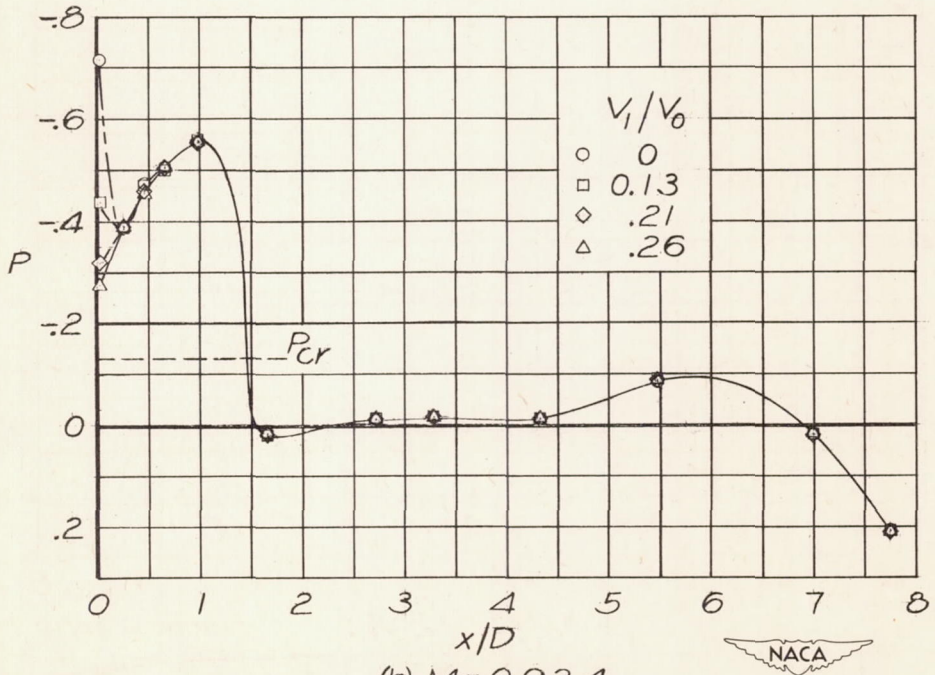

(b) $M_0 = 0.924$.

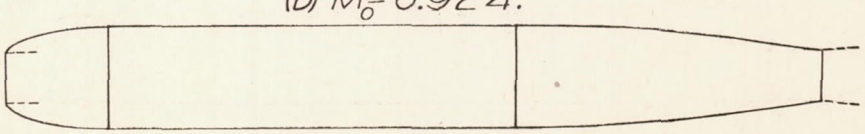

Figure 11.– Pressure distribution on NACA 1-50-100 nose inlet; $\alpha = 3.7^\circ$.

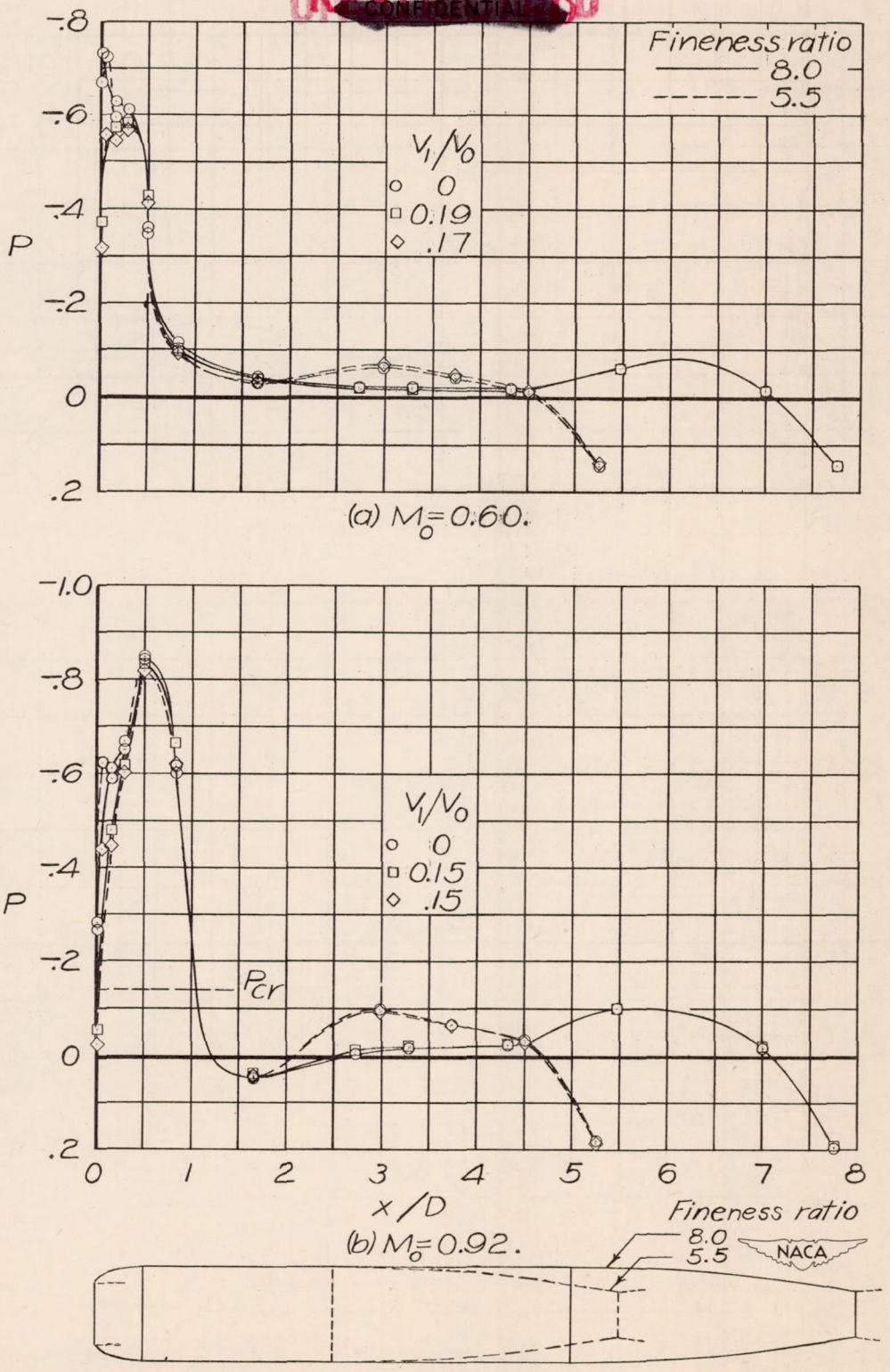

Figure 12.– Effect of fineness ratio on pressure distribution. NACA 1-65-050 nose inlet; $\alpha = 0^\circ$.

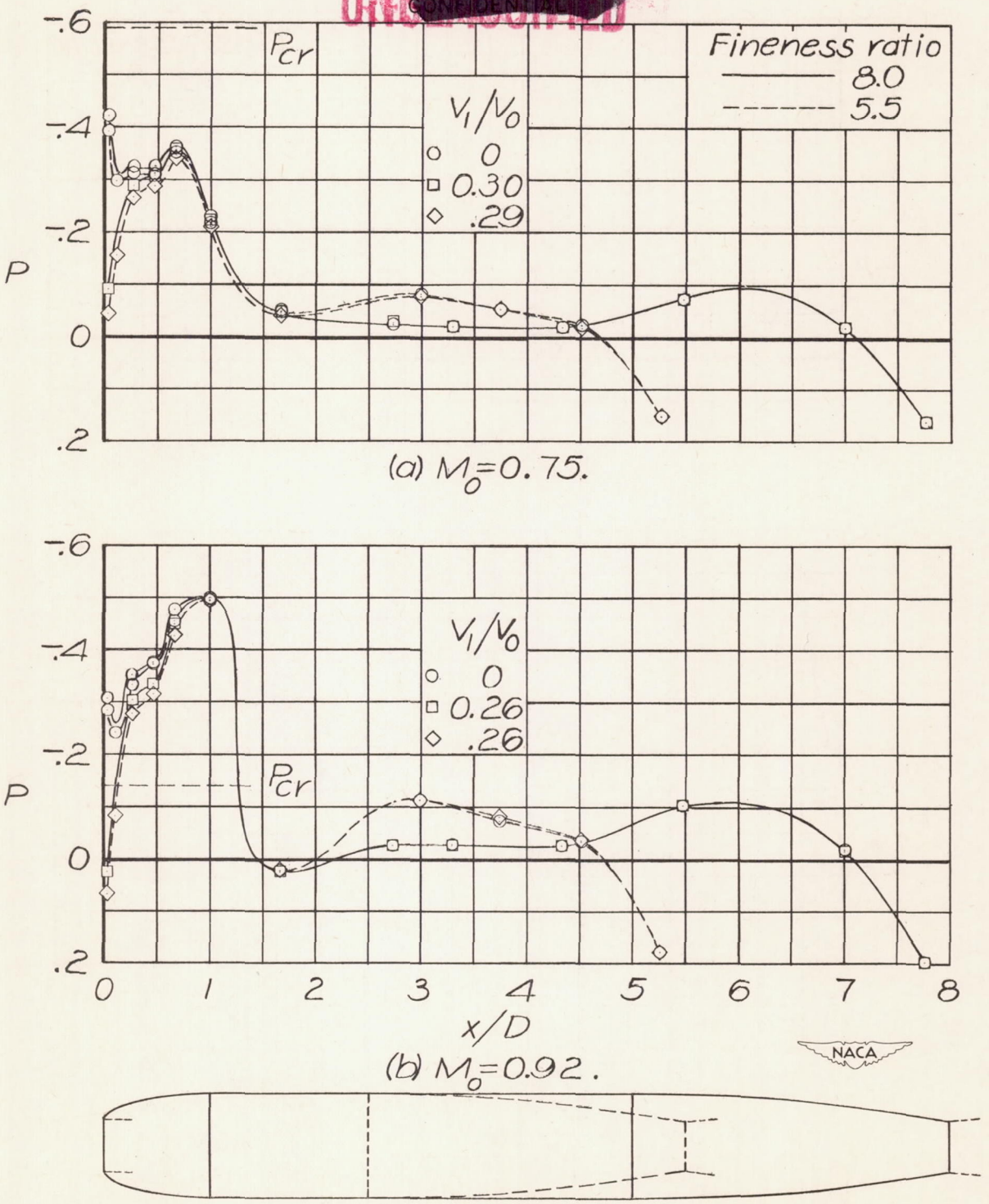

Figure 13.- Effect of fineness ratio on pressure distribution. NACA 1-50-100 nose inlet; $\alpha = 0^\circ$.

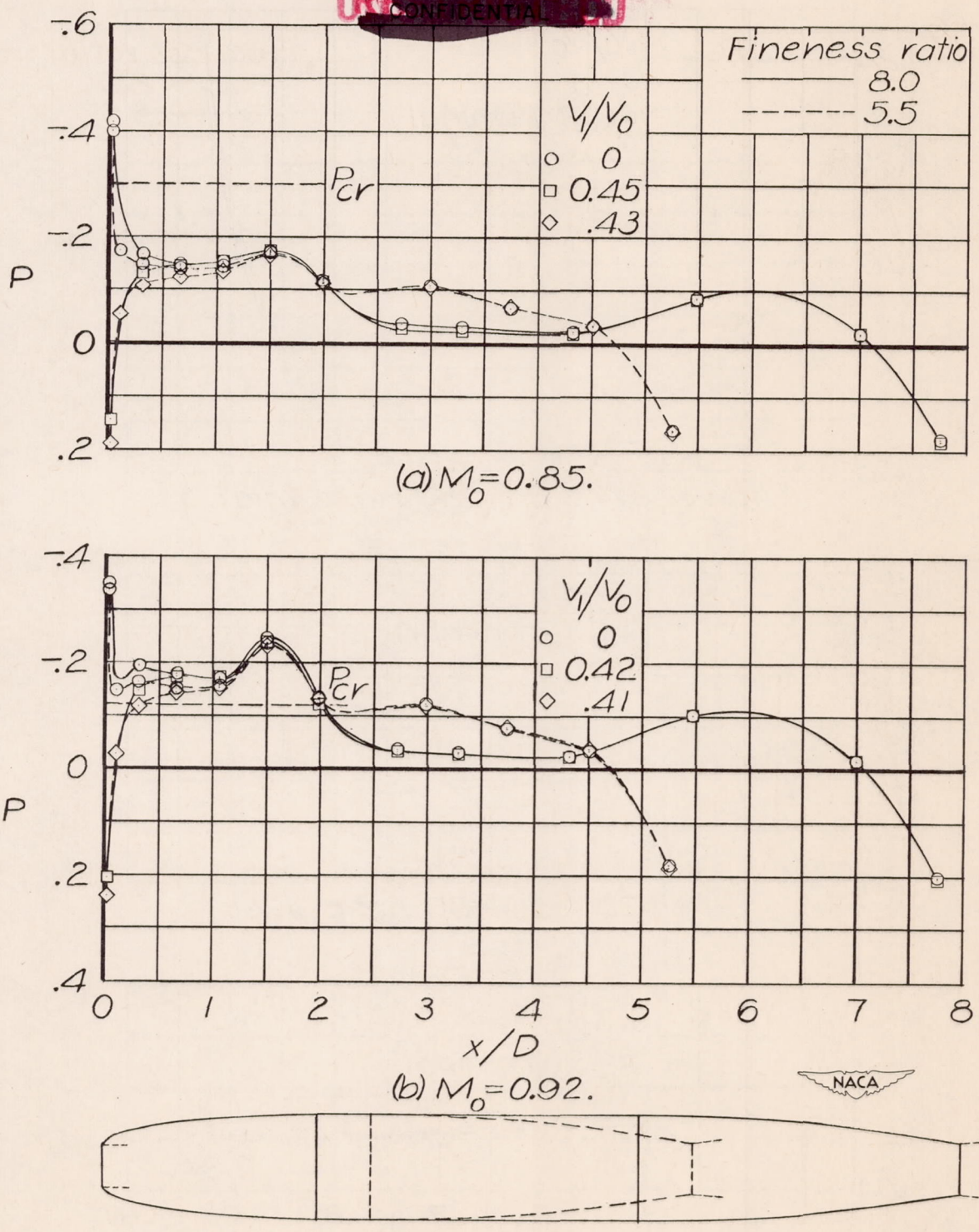

Figure 14.– Effect of fineness ratio on pressure distribution. NACA 1–40–200 nose inlet; $\alpha = 0^\circ$.

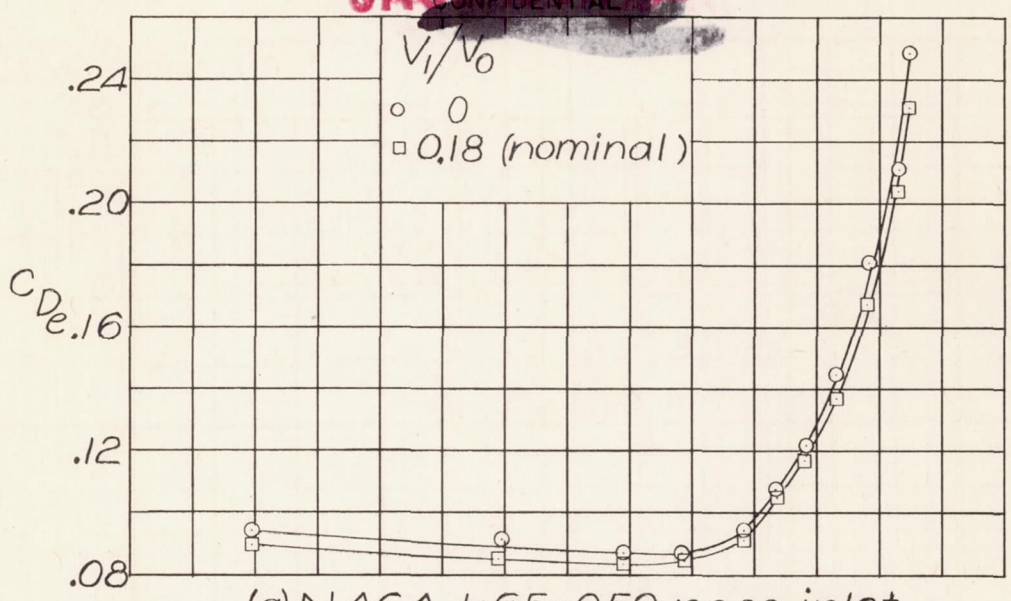

(a) NACA 1-65-050 nose inlet.

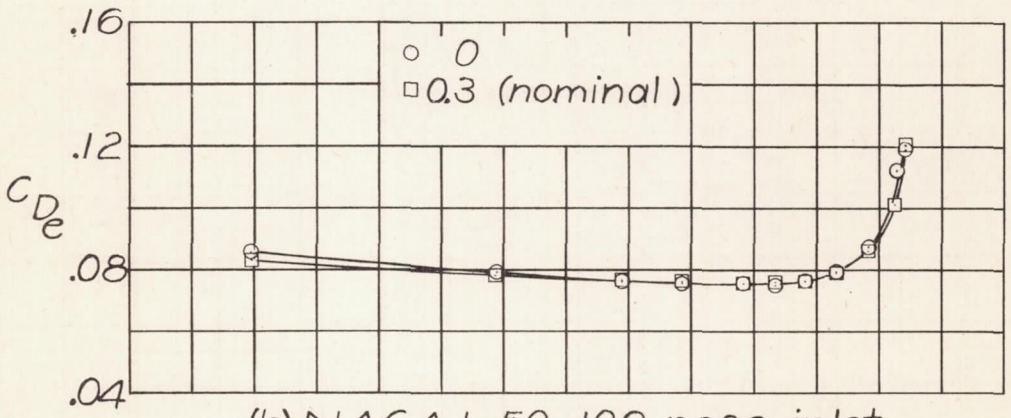

(b) NACA 1-50-100 nose inlet.

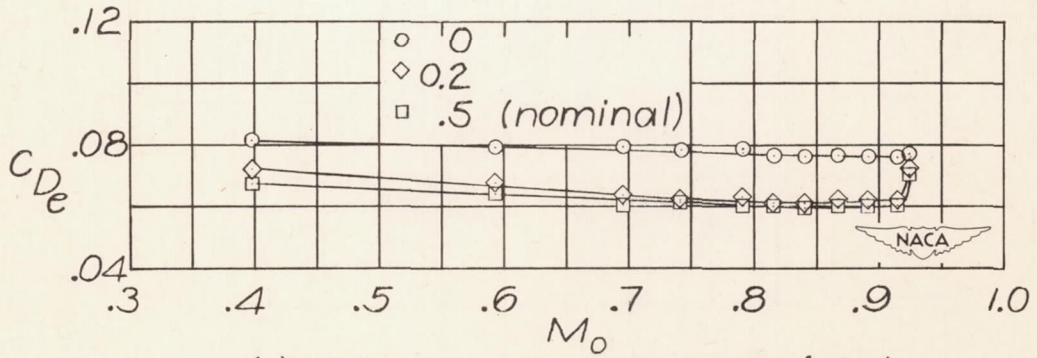

(c) NACA 1-40-200 nose inlet.

Figure 15.- Nose-inlet drag characteristics. $\alpha = 0^{\circ}$; fineness ratio 8.

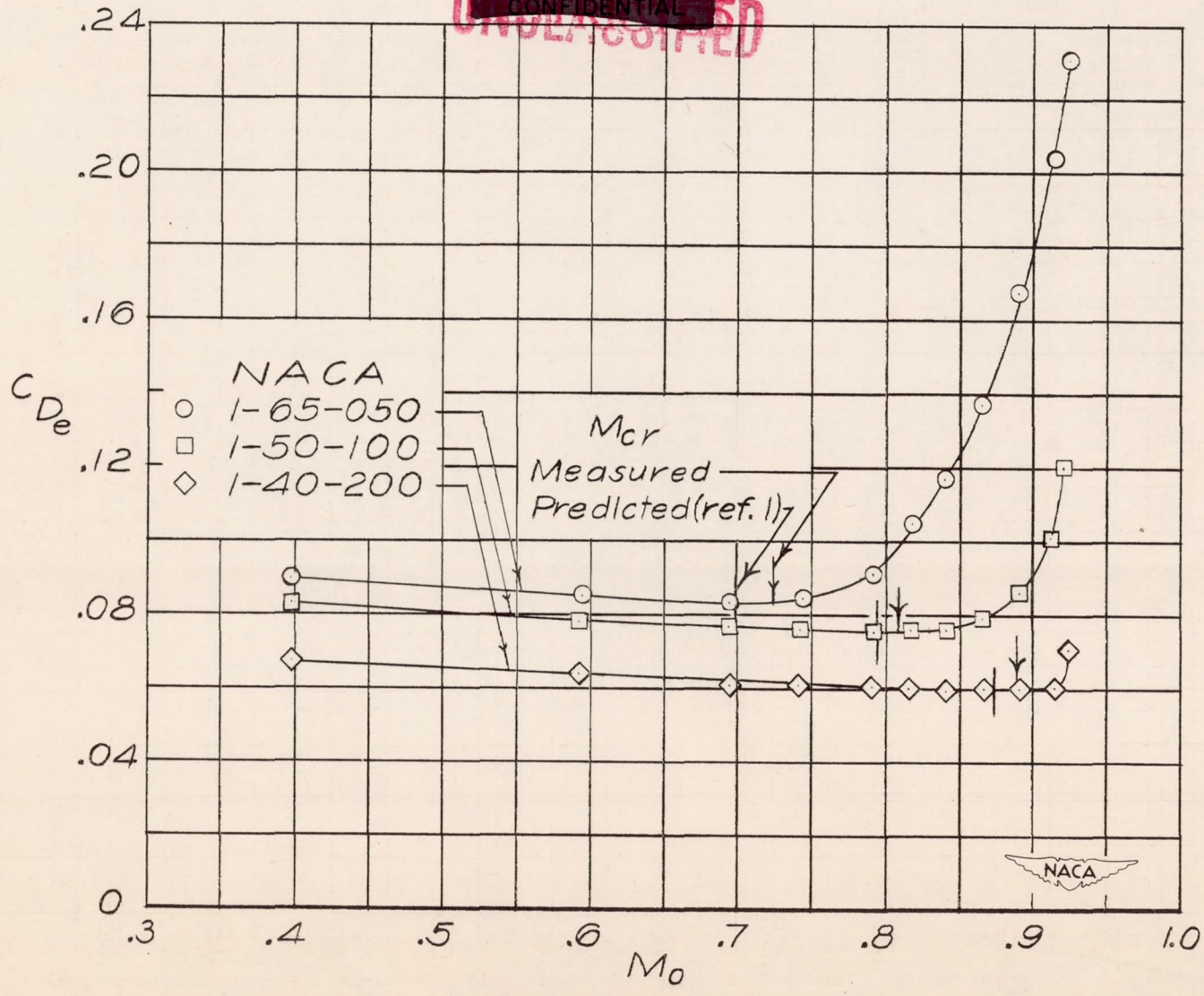

Figure 16.– Drag comparison of three nose inlets. $\alpha = 0^\circ$; maximum V_1/V_o; fineness ratio 8.

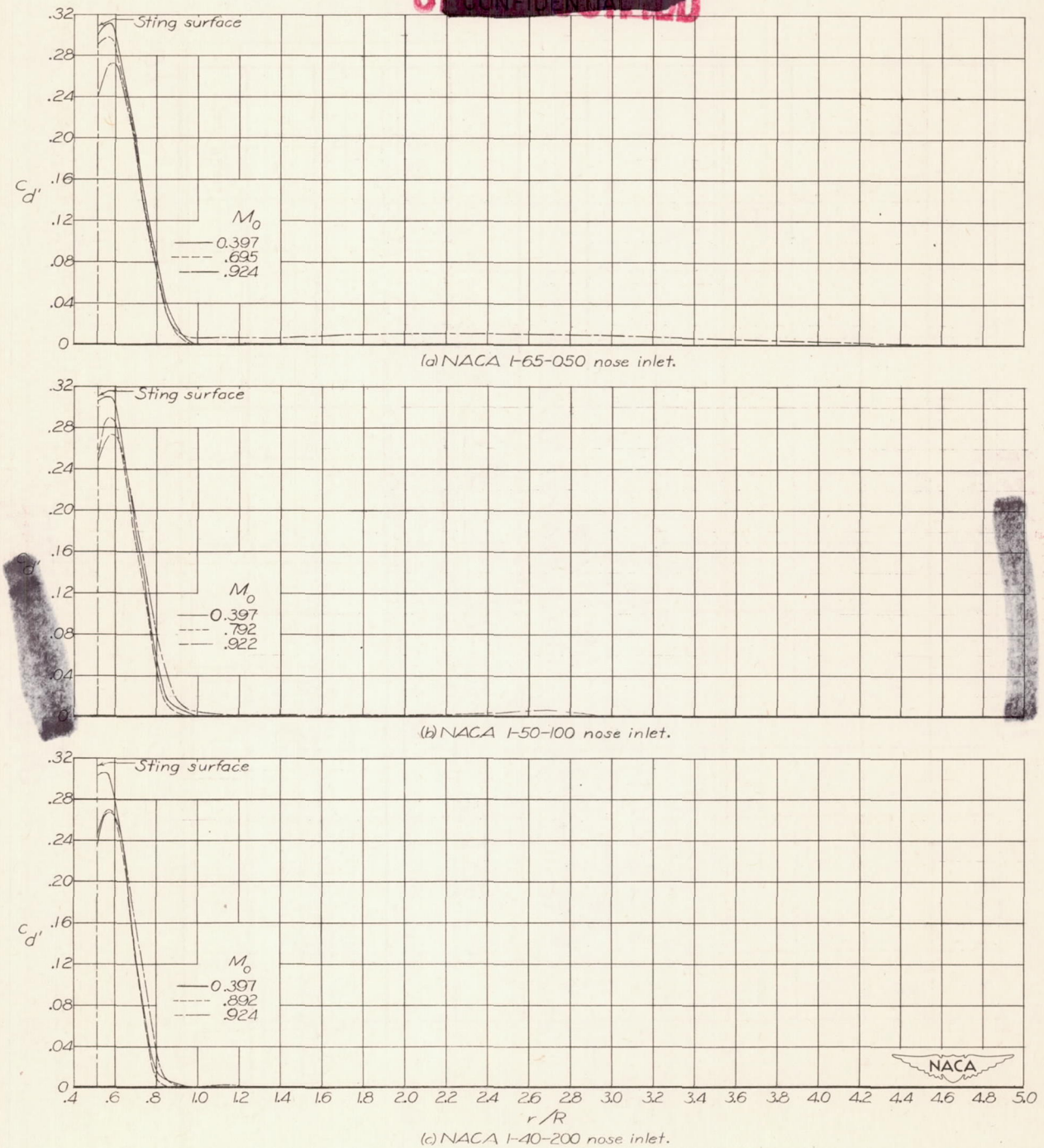

Figure 17.– Wake profiles. $\alpha = 0^{\circ}$; maximum V_1/V_o; fineness ratio 8.

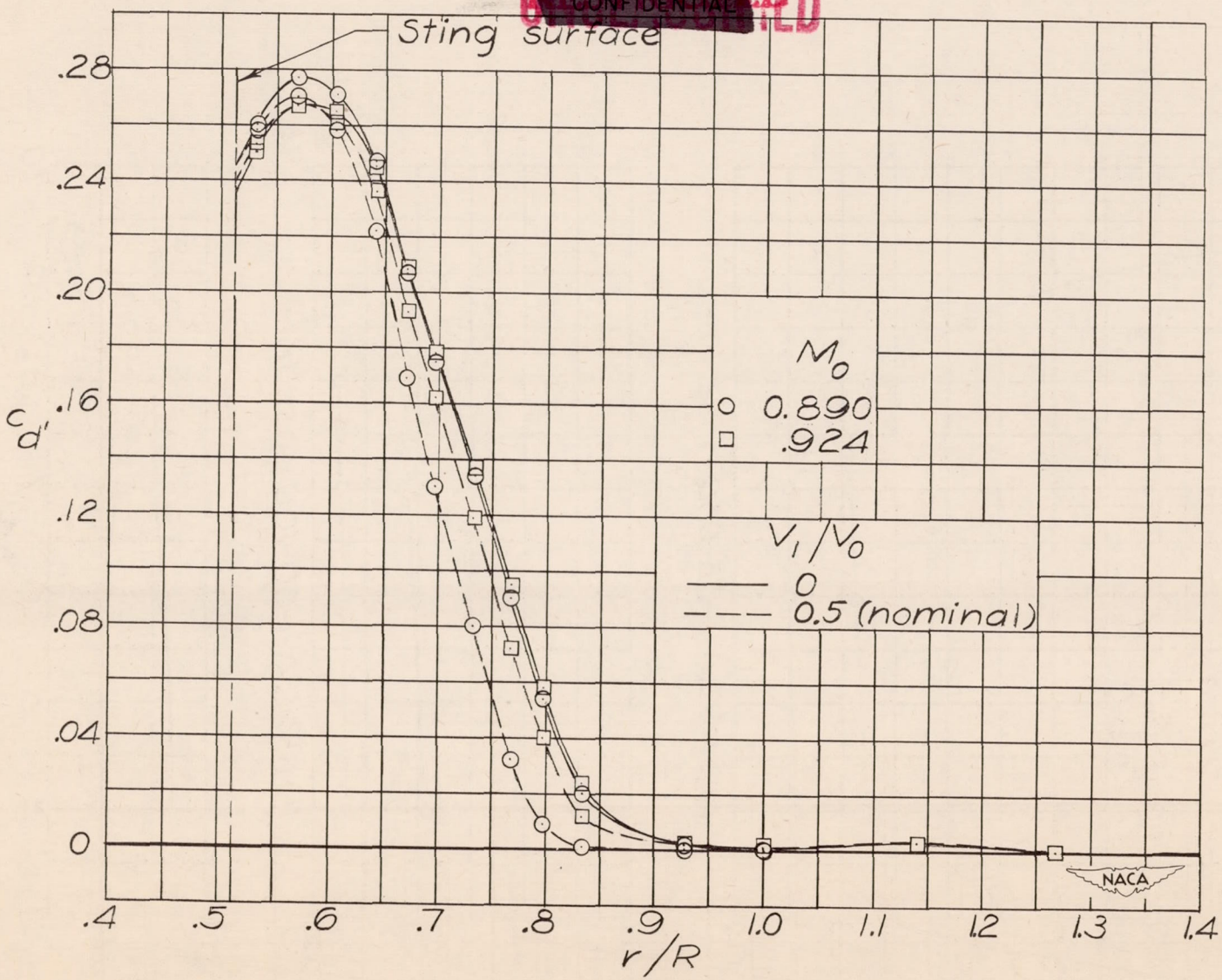

Figure 18.- Inlet-velocity ratio effects on wake profiles of NACA 1-40-200 nose inlet. $\alpha = 0°$.

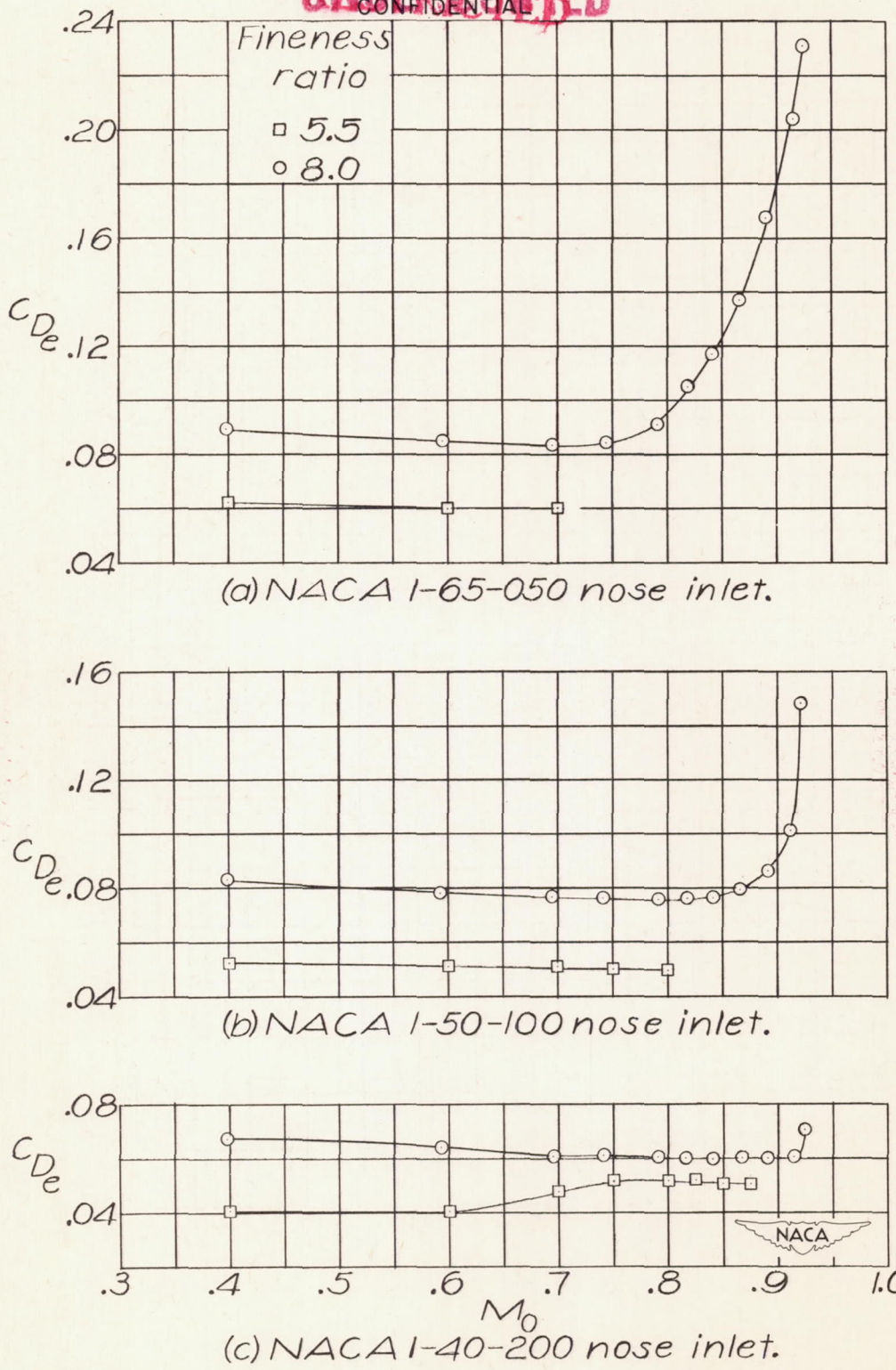

Figure 19.- Fineness-ratio effect on subcritical drag. $\alpha = 0^\circ$; maximum inlet-velocity ratio.

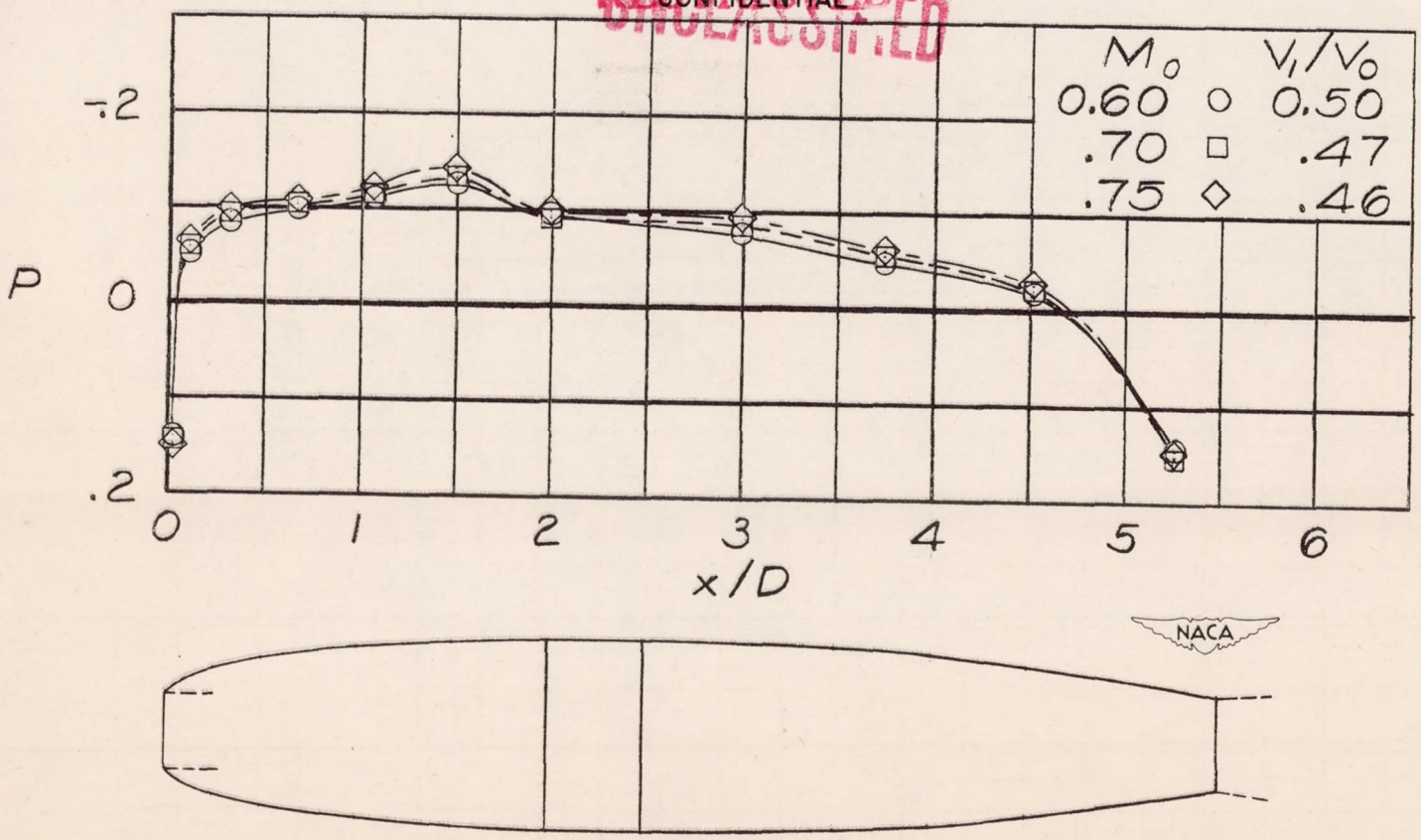

Figure 20.– Pressure distribution. NACA 1-10-200 nose inlet; $\alpha = 0^\circ$; maximum inlet-velocity ratio; fineness ratio 5.5.

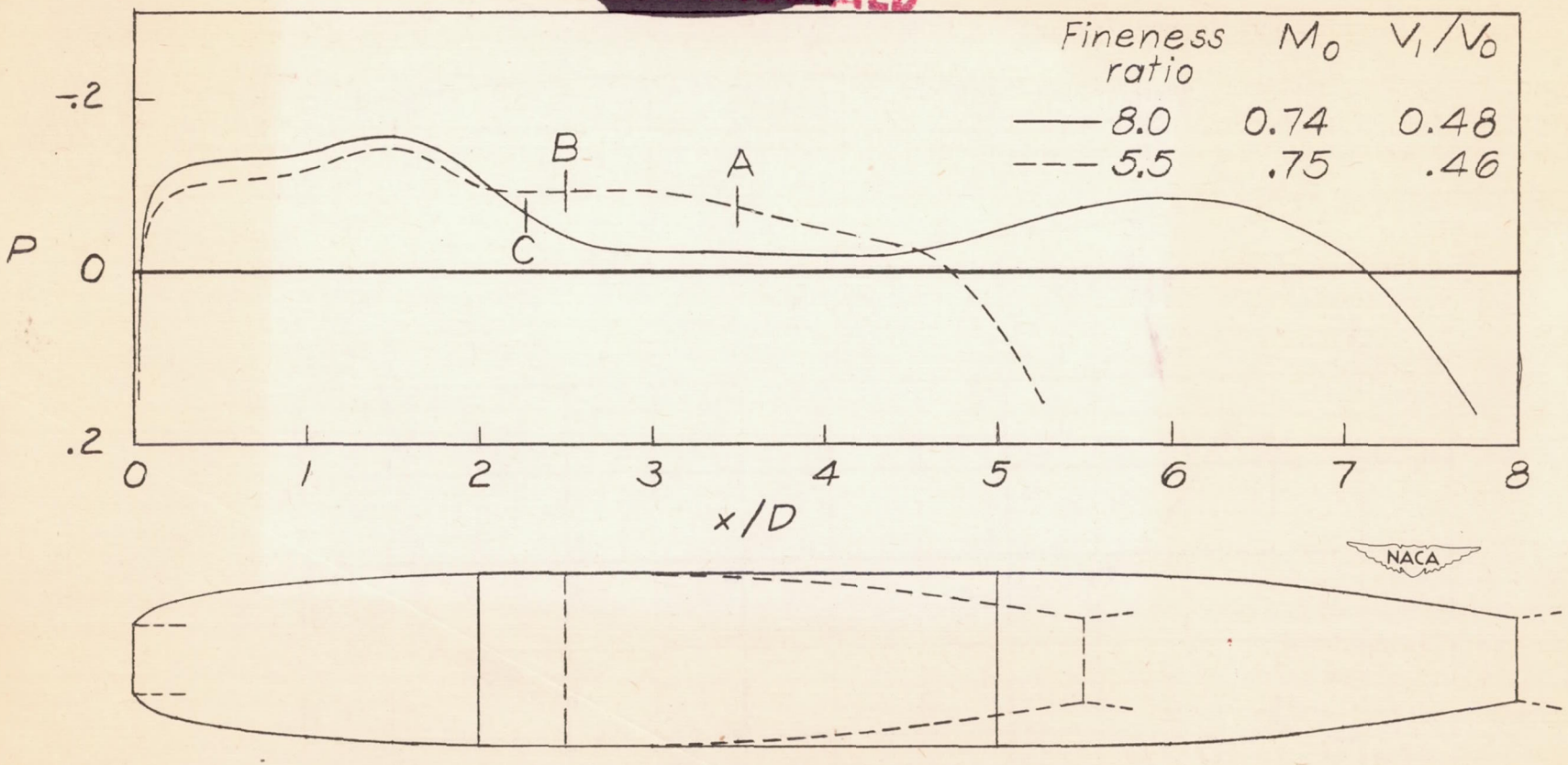

Figure 21.– Pressure distribution for two fineness ratios. NACA 1–40–200 nose inlet; $\alpha = 0^{\circ}$; maximum inlet-velocity ratio.